DEEP NEURAL NETWORK & DYNAMIC FUNCTIONAL CONNECTIVITY ANALYSIS OF FUNCTIONAL MRI DATA

by

Amaresh Kumar Mishra, BS

THESIS

Presented to the Faculty of

The University of Houston-Clear Lake

In Partial Fulfillment

Of the Requirements

For the Degree

MASTER OF SCIENCE

in Computer Engineering

THE UNIVERSITY OF HOUSTON-CLEAR LAKE

MAY, 2022

DEEP NEURAL NETWORK & DYNAMIC FUNCTIONAL CONNECTIVITY ANALYSIS OF FUNCTIONAL MRI DATA

by

Amaresh Kumar Mishra

APPROVED BY

_____

Unal ‘Zak’ Sakoglu, PhD, Committee Chair

_____

Hisham Al-Mubaid, PhD, Committee Member

_____

Jiang Lu, PhD, Committee Member

RECEIVED/APPROVED BY THE COLLEGE OF SCIENCE AND ENGINEERING:

_____

David Garrison, PhD, Associate Dean

_____

Miguel A Gonzalez, PhD, Dean

Dedication

I would like to dedicate this thesis to my late grandparents. They have been constant encouragement in my life.

Acknowledgements

I would like to thank my thesis advisor Dr. Unal ‘Zak’ Sakoglu for all his support on this work. I would like to thank him for being supportive and understanding throughout the entire time. He has given me a wonderful opportunity in the field of machine learning and brain magnetic resonance imaging data analyses.

I would like to acknowledge my thesis committee members Dr. Jiang Lu and Dr. Hisham Al-Mubaid for helping me with their input and comments. I would also like to extend my gratitude to Andrew James Hughes who has helped me during this project. I wish to extend my thanks to all the UHCL staff that contributed to this project. Finally, I would like to thank my family and friends who supported and encouraged me during difficult times.

ABSTRACT

DEEP NEURAL NETWORK & DYNAMIC FUNCTIONAL CONNECTIVITY ANALYSIS OF FUNCTIONAL MRI DATA

Amaresh Kumar Mishra
University of Houston-Clear Lake, 2022

Thesis Chair: Unal 'Zak' Sakoglu, PhD

This thesis work presents a dynamic functional connectivity (DFC)-based classification analysis of an already collected and completely de-identified functional magnetic resonance imaging (fMRI) dataset from two groups, veterans with Gulf War Illness (GWI), vs matched controls. Neuroimaging or brain imaging is the use of various techniques to either directly or indirectly image the structure, function, or pharmacology of the nervous system. fMRI is a neuroimaging technique which is used to measure brain activity by detecting changes associated with blood oxygenation level dependence (BOLD), which is an indirect measure of neural activity, and it helps obtain three spatial dimensional (3D) brain activation maps associated with certain stimulus and/or a task, depending on the experiments performed during the fMRI scan. Whole-brain resting-state fMRI (rsfMRI) data which were scanned from 23 GWI veterans (mean age 49.4) and 30 normal control (NC) veterans (mean age 49.8) were used for analyses. A computational method using DFC features, deep learning, and machine learning techniques were used to correctly classify GWI vs NC. Results show that, support vector machine (SVM) -based machine learning technique, combined with simple *t*-test method for feature extraction (using the DFC), performed better than convolutional neural network (CNN) deep learning method, in

terms of classification accuracy (upwards of 98% accuracy for the former vs. upwards of 60% accuracy for the latter).

TABLE OF CONTENTS

LIST OF TABLES

LIST OF FIGURES

CHAPTER I:

INTRODUCTION

Human brain research is among the most complex areas of study for scientists. It is known that aging and other factors, such as brain disorders, can affect brain structure and function, but more research is needed into what specifically occurs within the brain. Neuroimaging, or brain imaging, is the use of different techniques to either directly or indirectly image the structure, function, or pharmacology of the nervous system. With much of the research using magnetic resonance imaging (MRI) scans, data scientists are well-positioned to support future insights into the human brain, its functioning, and the way it is affected by various disorders and diseases [1].

Neuroimaging can be mainly classified into structural imaging and functional imaging. Structural neuroimaging is used for studying the structure of the nervous system and for the diagnosis of certain diseases such as brain tumors. Functional neuroimaging, on the other hand, is used for studying the functioning of the brain under different conditions and diseases such as mental disorders. This is done by tracking the dynamics of neural activity or neurovascular activity [2]. Functional magnetic resonance imaging (fMRI) is one of the most versatile non-invasive functional neuroimaging methods, which has been utilized over the past three decades to evaluate the effect of brain strokes, and to guide treatments [3]. It is a specialized form of MRI that uses the functional anatomy of the brain.

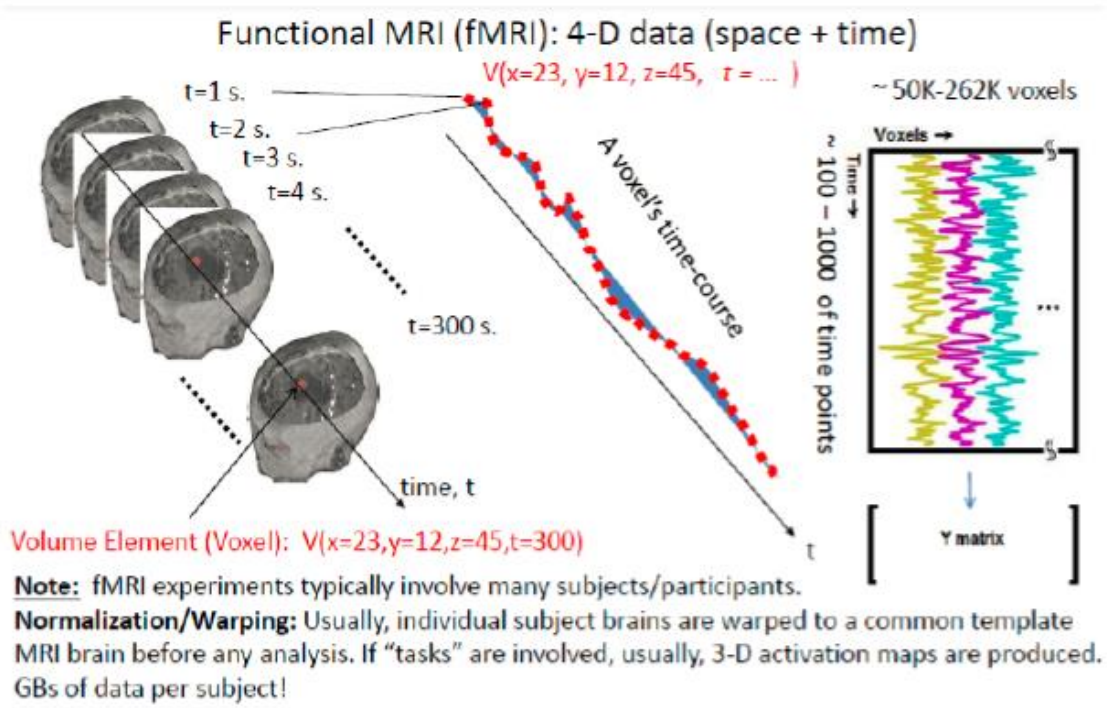

Figure 1: Visualization of functional MRI (fMRI), 4-D data (3-D space and time) [4].

A large amount of fMRI data from humans and animals have been collected by researchers to study the functioning of brain under various conditions, which include different stimuli and/or tasks that the participants were engaged with during the scans. Different types of advanced analysis methodologies have also been developed for fMRI data. This master's thesis work taps on some of these recently developed methodologies, using an already collected, completely de-identified fMRI data from two groups of subjects, Gulf War Illness (GWI) subjects and matched healthy control veterans. For this work, functional magnetic resonance imaging data, which was collected as part of a larger study at another institution, UT-Southwestern Medical Center in Dallas, TX, were utilized.

1.1 Functional Connectivity (FC):

FC has been characterized by the connectivity among different brain regions. Specifically, it is defined as temporal correlation between spatially remote neurophysiological events. That means two brain regions are considered to show functional connectivity if there is a statistical relationship between the measures of activity recorded for both of them [5]. This is applicable in both resting-state fMRI and task fMRI studies. While FC can refer to correlations across

subjects, runs, blocks, trials, or individual time points, resting-state FC functional connectivity focuses on connectivity assessed across individual BOLD time points during resting conditions [6]. Functional connectivity MRI (fcMRI), which can include resting-state fMRI and task-based MRI, might help provide more definitive diagnoses for mental health disorders such as bipolar disorder, and may also aid in understanding the development and progression of post-traumatic stress disorder (PTSD). Furthermore, it evaluates the effect of treatment [7] [8]. It is an expression of the network behavior underlying high-level cognitive function, partially unlike structural connectivity, as, structural connectivity looks for a physical connection between brain regions [8]. Since the brain is a highly dynamic system, functional connectivity has been shown to change on the order of seconds by analyses of dynamic functional connectivity [9].

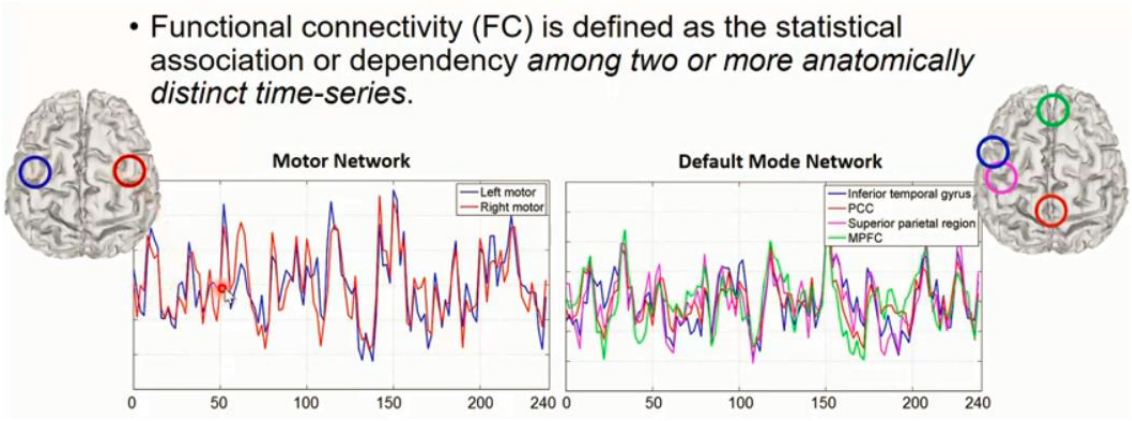

Figure 2: Pictorial representation of defining functional connectivity [10].

1.2 Dynamic Functional Connectivity (DFC):

Dynamic functional connectivity (DFC) can be defined as functional connectivity (FC) of brain regions or networks over a relatively short period, when compared to the duration of the whole fMRI scan/experiment. DFC captures functional connectivity changes over a short time window [11, 12, 13]. DFC is a recent expansion on traditional FC analysis which typically assumes that functional networks are static in time. DFC analyses have been applied to different neurological disorders and have been suggested to be a more accurate representation of the behavior of functional brain networks [14, 15]. The primary neuroimaging application of DFC is

fMRI, but DFC can also be applied to other functional neuroimaging data with time-varying signals, such as electroencephalography (EEG) [16, 17]. DFC is a relatively recent development within the field of functional neuroimaging whose discovery was motivated by the observation of temporal variability in the rising field of steady-state connectivity research [14, 18, 19].

1.2.1 Types of Analysis Technique:

Sliding window DFC Analyses: Sliding window DFC analysis is the most common method used in the analysis of functional connectivity, first introduced by Sakoglu and Calhoun in 2009, which was applied to schizophrenia [15, 18, 19]; since it was applied in conjunction with independent component analysis (ICA) which leads to brain "networks", it was dubbed "dynamic functional network connectivity". Sliding window analysis is performed by conducting analysis on a set number of scans in an fMRI session. The number of scans included is the length of the sliding window. The defined window is then moved a certain number of scans forward in time and additional analysis is performed. The movement of the window is usually referenced in terms of the degree of overlap between adjacent windows [20].

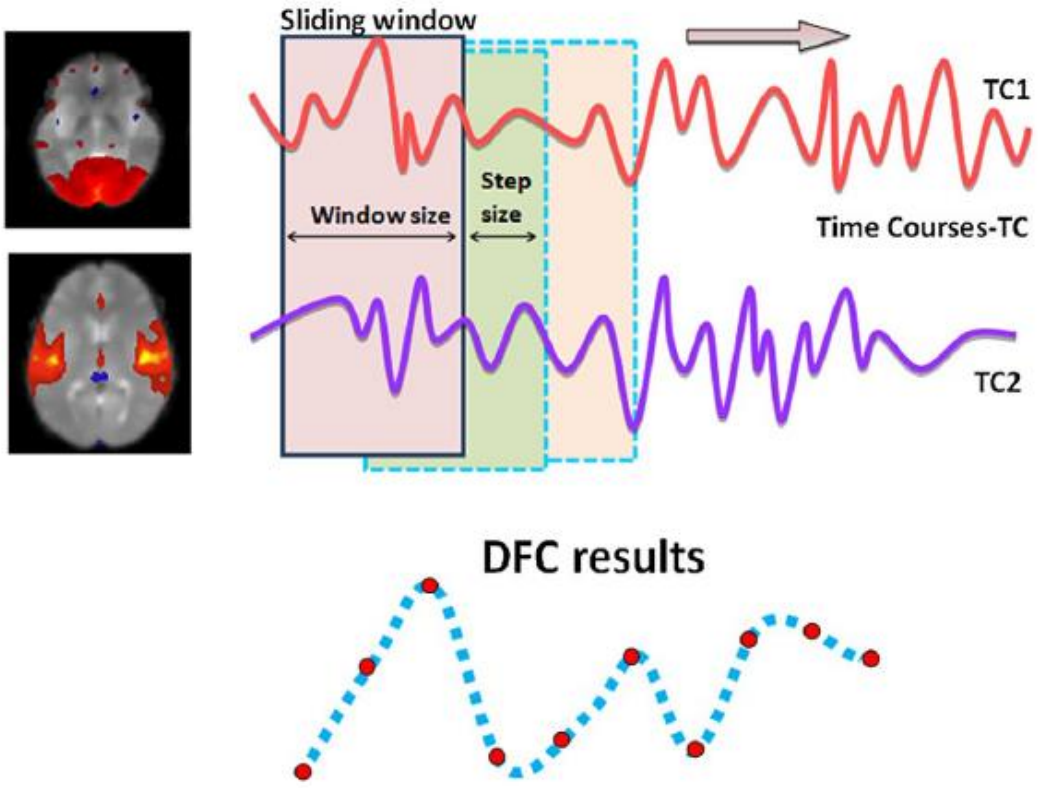

Figure 3: Visualization of Dynamic Functional Connectivity (DFC) analysis on two brain regions. The two brain regions, each with their fMRI time course, constitute a "pair". For each pair, and for each time window, one DFC time point is obtained. By sliding the time window, the DFC time course for the pair is obtained [20].

One of the principal benefits of sliding window analysis is that almost any steady-state analysis can also be performed using sliding window if the window length is sufficiently large. This analysis has a benefit of being easy to understand and in some ways easier to interpret [21]. As the most common method of analysis, sliding window analysis has been used in many ways to investigate a variety of characteristics and implications of DFC. To be accurately interpreted, data from sliding window analysis generally must be compared between two different groups. Researchers have used this type of analysis to show different DFC characteristics in diseased and healthy patients, high and low performers on cognitive tasks, and between large-scale brain states.

Activation patterns: One of the first methods ever used to analyze DFC was pattern analysis of fMRI images which shows the patterns of activation in spatially separated brain

regions that tend to have synchronous activity. This makes it clear that there is a spatial and temporal periodicity in the brain that probably reflects some of the constant processes of the brain [22]. Repeating patterns of network information have been suggested to account for 25–50% of the variance in fMRI BOLD data [23, 24, 25]. Patterns of activity have primarily been seen in rats as a propagating wave of synchronized activity along the cortex. These waves have also been shown to be related to underlying neural activity and have been shown to be present in humans and rats [24].

Point process analysis: Departing from the traditional approaches, recently an efficient method was introduced to analyze rapidly changing functional activation patterns which transform the fMRI BOLD data into a point process [25, 26]. This is achieved by selecting for each voxel, the points of inflection of the BOLD signal (i.e., the peaks). These few points contain most of the information pertaining to functional connectivity because, it has been demonstrated that, despite the tremendous reduction on the data size (> 95%), it compares well with inferences of functional connectivity [27, 28] obtained with standard methods, which uses the full signal.

The large information content of these few points is consistent with the results of Petridou et al. [29], who demonstrated the contribution of "spontaneous events" to the correlation strength and power spectra of the slow spontaneous fluctuations by deconvolving the task hemodynamic response function from the rest data. Subsequently, similar principles were successfully applied under the name of co-activation patterns (CAP) [30, 31].

Other methods: Time-frequency analysis has been proposed as an analysis method that can overcome many of the challenges associated with sliding windows. Unlike sliding window analysis, time-frequency analysis allows the researcher to investigate both frequency and amplitude information simultaneously. The wavelet transform has been used to conduct DFC analysis that has validated the existence of DFC by showing its significant changes in time. This same method has recently been used to investigate some of the dynamic characteristics of accepted networks. For example, time-frequency analysis has shown that the anticorrelation between the default mode network and the task-positive network is not constant in time but

rather is a temporary state [32]. Independent component analysis (ICA) has become one of the most common methods of network generation in steady-state functional connectivity. Spatial ICA divides fMRI signal into several spatial components that are spatially statistically independent, but have similar temporal patterns within. Recently, ICA has been also used to divide fMRI data into statistically independent temporal components, which has been termed temporal ICA, and it has been used to plot network behavior that accounts for 25% of the variability in the correlation of anatomical nodes in fMRI [33].

1.2.2 Clinical Importance:

The principal motivation of DFC analysis is that the brain function is highly dynamic; thus, DFC analysis tracks the dynamics of functional connectivity among different brain networks. Both static FC and DFC have been significantly helpful and related to a better understanding of the effects of a variety of diseases and disorders, including depression [33], cocaine-addiction [20], schizophrenia [34] and Alzheimer's disease [35]. For example, studies with Alzheimer's disease have shown that patients suffering from this ailment have altered network connectivity as well as altered time spent in the networks that are present [35]. The observed correlation between DFC and disease does not imply that the changes in DFC are the cause of any of these diseases, but information from DFC analysis may be used to better understand the effects of the disease and to diagnose them more quickly and accurately.

Exploratory analysis of ICA-based functional connectivity employing GWI veterans and veteran healthy controls yielded several significant insights into brain mechanisms underlying GWI [36]. The outcome of the experiment reveals that the impaired functional connectivity between brain function networks as a mechanism underlying GWI symptoms [36]. The results also provided strong evidence for the concept that GWI is indeed a disease of the brain, with rsfMRI results confirming self-reported symptoms and neurocognitive assessments in several functional domains [36].

1.3 Problem Statement:

Approximately 250,000 U.S. veterans out of almost 700,000 who were deployed in the 1991 Gulf War (GW) are affected by a chronic multi-symptom illness, a condition with serious consequences called GW illness (GWI), which is characterized by multiple deficits in cognitive, affective, sensory and nociception domains [36]. In this study data used is already-collected and completely de-identified resting-state fMRI (rsfMRI) data from GWI to apply deep neural network learning methods and dynamic functional connectivity methods to find the most discriminating brain networks or regions (GWI vs matched controls) and thus finding some of the involved functional brain regions or networks function in GWI. Prior works found impaired functional connectivity (FC) in GWI veterans among several brain function networks consistent with their self-reported symptoms, for example, they exhibited impaired FC between language networks and sensory input networks of all modalities as well as motor output networks and also showed impaired FC between different sensory perception and motor networks, and between different networks in the sensorimotor domain [36]. These FC impairments provide a putative mechanism of central nervous system dysfunction in GWI. We utilized fMRI data from these networks to construct features and perform deep neural net-based and SVM classification.

CHAPTER II:

BACKGROUND WORKS

About one-third of those deployed in the 1991 Gulf War (GW) suffer from GW illness (GWI). Since the war, GW veterans have shown higher than-average rate of developing certain sign or symptoms which cannot be explained by any specific medical problems. The symptoms include (In addition to what explained in Section 1.3) “Sustained and Debilitating Fatigue”, “Headache and Migraines”, “Difficult Sleeping”, “Problems with Memory and Cognition” and “Digestive Ailments” [37].

2.1 Demographics and Clinical Characteristics of the Samples [36]:

Demographics and other clinical characteristics of the objects are listed below. The below list suggests that there were no significant differences in age and education between GWI and military controls. These demographics in the table refer to the larger dataset where GWI patients from three different symptom groups were combined; in this thesis work, we only used GWI “Symptom-2” data group (n=23), from the GWI patients who report the symptoms with the most severity.

Table 1:

Demographics and Clinical Characteristics of 60 from Gulf War Imaging and 30 Matched Control [2].

Demographics and Clinical Characteristics	**GWI (60 Participants)**	**NC (30 Participants)**
Age in Years	50.1 ± 8	50.0 ± 8
Education in Years	5.2 ± 2	5.3± 2
Gender(F/M)	15	6
Right-handed in Sample	57	29
CDC GWI Case Definition	60	0
Modified Kansas GWI Case Definition	60	0
Chronic Fatigue Syndrome	6	0
Fibromyalgia	34	0
PTSD	24	0
Other Mood Disorders	40	3

In this study, we have used already collected and completely de-identified resting-state fMRI (rsfMRI) data from GWI to apply deep neural network learning methods, support vector machine and dynamic functional connectivity methods to find the most discriminating brain networks or regions (GWI vs matched controls) and thus finding some of the involved functional brain regions or networks function in GWI. Prior works found impaired functional connectivity (FC) in GWI veterans among several brain function networks consistent with their self-reported symptoms. For example, they exhibited impaired FC between language networks and sensory input networks of all modalities as well as motor output networks and showed impaired FC between different sensory perception and motor networks, and between different networks in the sensorimotor domain [36]. These FC impairments provide a putative mechanism of central nervous system dysfunction in GWI. We utilized fMRI data from these networks to construct features and perform deep neural-net based and SVM classification.

Let us begin with the underlying basics of DFC algorithm. DFC- based analysis involves windowed correlation operation over time courses of the brain signals [38].

2.2 Understanding the AAL ATLAS region average DFC:

Using the pseudocode below, we have calculated the region average DFC matrices for the two groups and used them in the following sections.

Pseudocode

```
Input
GWIRawData  = This variables stores all the53 subjects' raw imaging data.
numOfSubj = length(GWIRawData)
WindowLenght = 32
StepSize = 8
NumRegion = 116 (The AAL Atlas has 116 brain regions)
AalUtility = 3mm_SPMresliced_aal.nii
reSlicedAAL = spm_read_vol(spm_vol(GWIRawData, 3mm_SPMresliced_aal.nii)
for i = 1:numOfSubj
   subjectNiiName=myFilenames(i).name
   my4Ddata=spm_read_vols(spm_vol(strcat(GWIRawData,subjectNiiName)))
  [m n k] = size(reSlicedAAL )
  for a=1:NumRegion
     for b = 1:m
        for c = 1:n
           for d = 1:k
             if reSlicedAAL (a,b,c) ==1
              tempsignal = squeeze(my4Ddata);
              finsignal = [finsignal tempsignal];
             end
           end
```

```
        end
      end
finavgsignal = median(finsignal);% calculate the median ignoring nulls.
finROIfc = correlation(finavgsignal);
  %This is the DFC loop
  for iw = 1:numWindows
      myavgsignal_window = finavgsignal (:,(iw-1)×stepSize+1:(iw-
1)×stepSize+windowLength); %changed from myavgsignal to _allsubjects
      finalROIfc_window = corr(myavgsignal_window');
      finalROIDfc_allsubjects(is, :, :, iw)=myROIfc_window;
  end

end
```

CHAPTER III:

METHODS AND MATERIALS

A relatively recently developed fMRI analysis method is dynamic functional connectivity, which performs dynamic, temporally-evolving interactions among different brain networks [11]. DFC analyses also generate enormous amount of features. These features can be utilized by machine learning algorithms as well as more-recently developed deep learning algorithms. In this thesis, we performed DFC analysis on an already collected, de-identified and pre-processed fMRI data from Gulf War Illness [36]. We have performed DFC analyses, extracted DFC features and fed them into different machine learning algorithms including deep neural network algorithms to perform the classification of subjects and execute extensive cross-validation to evaluate methodologies and identify the most-discriminating brain networks or regions.

The analyses and programming were mainly done and implemented using MATLAB scientific programming language since it provides a great programming environment including Deep Learning tools.

GWI data analysis was performed and converted into 4D dimensional MATLAB-readable format files (.mat). These data were further divided into four categories such as, Controls, Syndrome 1, Syndrome 2 and Syndrome 3. Each category has been given a label from zero to three. Label zero is assigned to ‘control veterans’ and we call it “group zero”, label two is ‘Syndrome 2’, called “group two”. In this research our goal was to find out the best possible method to classify group zero vs group two.

In this work our data set is 4D (number of object in a group x Number of Brain Regions x Number of Brain Regions x Windows). The total number of features of the dataset is close to half a million. Handeling such a huge number of features was a challenging part. In this process we mainly focussed to utlize R-CNN and SVM on DFC data set. Furthermore, to draw the conlusion, same methods have been utilized on FC data set. In this research work MATLAB and

its funtions have been used for all of the aforementioned methods. Details of each method are explained below.

3.1 Classification using R-CNN:

It begins by applying selective search to extract region-of-interest (ROI), where each ROI is a 3D shape which may represent the set of a specific brain region. Depending on the scenarios, there may be many ROIs. After that, each ROI is fed through neural network to produce output features [39].

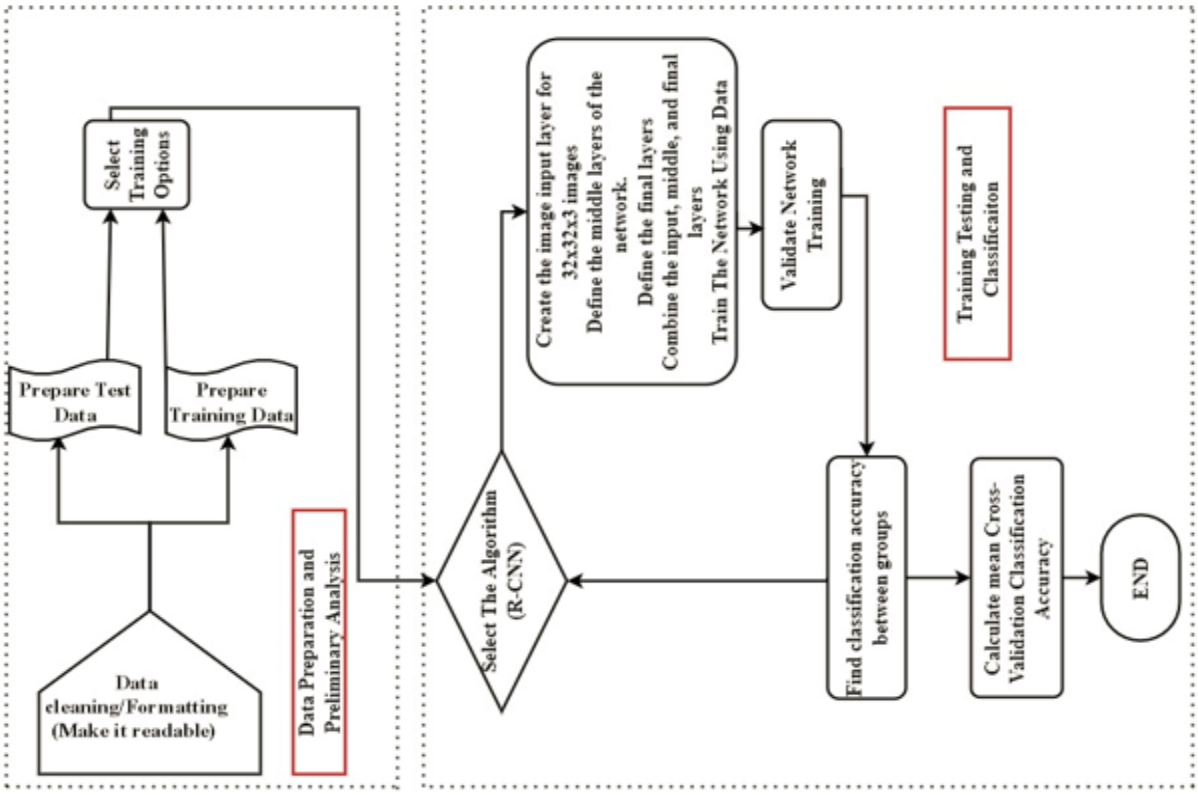

Figure 4: Proposed framework DFC Based Classification of GWI fmri data using R-CNN.

In this process after receiving the input data(image), goal is to first prepare training images and test images. Once training and test images are prepared, select the best possible training options available in MATLAB, such as sgdm, Momentum, InitialLearningRate, LearnRateSchedule etc. Details about training options have been explained below in the tabular form.

***Pseudocode*:**

training_images = [group_zero; group_two]

training_labels = [zeros(30,1), 2×ones(23,1)]

test_images = training_images

n = scalar

for i= 1:n

set aside some percentage of training images for validation.

set training options viz, sgdm, momentum, etc.

set input_layer

[height, width, numChannels] = size(training_image)

input_image_size = [height, width, numChannels]

input_layer = imageinputlayer(input_image_size)

set filter properties

set middle and final layer

combine all the layers defined above

train the network using "trainNetwork"

validate the network training

calculate the cross-validation accuracy in each cycle

end

calculate the mean cross-validation accuracy.

Table 2:

Training options name and descriptions [40].

Field	**Description**
sgdm	Stochastic gradient descent with momentum
Momentum	This parameter only applies if the solver is 'sgdm'. The momentum determines the contribution of the gradient step from the previous iteration to the current iteration of training. It must be a value between 0 and 1, where 0 will give no contribution from the previous step, and 1 will give a maximal contribution from the previous step. The default value is 0.9.
InitialLearnRate	The initial learning rate that is used for training. If the learning rate is too low, training will take a long time, but if it is too high, the training is likely to get stuck at a suboptimal result. The default is 0.01 for solver 'sgdm' and 0.001 for solvers 'adam' and 'rmsprop'.
LearnRateSchedule	This option allows the user to specify a method for lowering the global learning rate during training. Possible options include: - 'none' - The learning rate does not change and remains constant. - 'piecewise' - The learning rate is multiplied by a factor every time a certain number of epochs has passed. The multiplicative factor is controlled by the parameter 'LearnRateDropFactor', and the number of epochs between multiplications is controlled by 'LearnRateDropPeriod'. The default is 'none'.
LearnRateDropFactor	This parameter only applies if the 'LearnRateSchedule' is set to 'piecewise'. It is a multiplicative factor that is applied to the learning rate every time a certain number of epochs has passed. The default is 0.1.
LearnRateDropPeriod	This parameter only applies if the 'LearnRateSchedule' is set to 'piecewise'. The learning rate drop factor will be applied to the global learning rate every time this number of epochs is passed. The default is 10.
L2Regularization	The factor for the L2 regularizer. Itshould be noted that each set of parameters in a layer can specify a multiplier for this L2 regularizer. The default is 0.0001.
Epoch	Epoch number. An epoch corresponds to a full pass of the data.

Field	Description
MaxEpochs	The maximum number of epochs that will be used for training. The default is 30.
MiniBatchSize	The size of the mini-batch used for each training iteration. The default is 128.
Verbose	If this is set to true, information on training progress will be printed to the command window. The default is TRUE.
Iteration	Iteration number. An iteration corresponds to a mini-batch.
Time Elapsed	Time elapsed in hours, minutes, and seconds.
Mini-batch Accuracy	Classification accuracy on the mini-batch.
Validation Accuracy	Classification accuracy on the validation data. If you do not specify validation data, then the function does not display this field.
Mini-batch Loss	Loss on the mini-batch. If the output layer is a ClassificationOutputLayer object, then the loss is the cross-entropy loss for multi-class classification problems with mutually exclusive classes.
Validation Loss	Loss on the validation data. If the output layer is a ClassificationOutputLayer object, then the loss is the cross-entropy loss for multi-class classification problems with mutually exclusive classes. If you do not specify validation data, then the function does not display this field.
Base Learning Rate	Base learning rate. The software multiplies the learn rate factors of the layers by this value.

Below are some training options along with the training parameter values that were selected during this process. Please note, training options have been selected and optimized looking at the results. The below list of training options values contains sample values, that have been used to get the results. During this process, many other ‘training options’ combinations have been used. Out of those training options, the below are the optimized ones.

Table 3:

Training options value set 1.

Training Options	**Value**
sgdm	Plots, training-progress
Momentum	0.9
InitialLearnRate	0.01
LearnRateSchedule	piecewise
LearnRateDropFactor	0.1
LearnRateDropPeriod	8
L2Regularization	0.004
ValidationFrequency	15
MaxEpochs	20
MiniBatchSize	9
ValidationData	Xvalidation, Yvalidation
Verbose	TRUE

Table 4:

Training options value set 2.

Training Options	**Value**
sgdm	Plots, training-progress
Momentum	0.95
InitialLearnRate	0.015
LearnRateSchedule	piecewise
LearnRateDropFactor	0.1
LearnRateDropPeriod	8
L2Regularization	0.004
ValidationFrequency	15
MaxEpochs	20
MiniBatchSize	9
ValidationData	Xvalidation, Yvalidation
Verbose	TRUE

Table 5:

Training options value set 3.

Training Options	**Value**
sgdm	Plots, training-progress
Momentum	0.95
InitialLearnRate	0.015
LearnRateSchedule	piecewise
LearnRateDropFactor	0.1
LearnRateDropPeriod	8
L2Regularization	0.004
ValidationFrequency	15
MaxEpochs	24
MiniBatchSize	9
ValidationData	Xvalidation, Yvalidation
Verbose	TRUE

Once training options are set, and all the training and test data sets are segregated, the goal in this exercise was to create a convolutional neural network (CNN). A CNN is composed of a series of layers, where each layer defines a specific computation. MATLAB deep learning toolbox provides the functionality to easily design a CNN layer-by-layer. In this case, the following layers are used to create CNN.

inputLayer, middleLayers and finalLayers.

imageInputLayer - Image input layer defines an image input layer input size is the size of the input images for the layer. It must be a row vector of two or three numbers. During this work imageInputLayer is a three number vector consisting of height width and number of channels. It is defined as follows.

[height,width,numChannels, ~] = size(trainingImages).

imageSize = [height width numChannels].

inputLayer = imageInputLayer(imageSize)

middleLayers consists of convolutional2dLayer, reluLayer, maxPooling2dLayer

convolution2dLayer - 2D convolution layer for Convolutional Neural Networks. It is defined as follows.

Convolutional2dLayer. The first convolutional layer has a bank of 32 7x7x3 filters. Symmetric padding of 2 pixels is added to ensure that image borders are included in the processing. This is important to avoid information at the borders being washed away too early in the network

reluLayer - Rectified linear unit (ReLU) layer creates a rectified linear unit layer. This type of layer performs a simple threshold operation, where any input value less than zero will be set to zero.

maxPooling2dLayer - Max pooling layer creates a layer that performs max pooling. A max-pooling layer divides the input into rectangular pooling regions, and outputs the maximum of each region. poolSize specifies the width and height of a pooling region. It can be a scalar, in which case the pooling regions will have the same width and height, or a vector. It is defined as following during the classification process.

maxPooling2dLayer (3, 'Stride',2).

finalLayers consist of fullyConnectedLayer, reluLayer, softmaxLayer and classificationLayer.

fullyConnectedLayer is defined as it creates a fully connected layer output Size specifies the size of the output for the layer. A fully connected layer will multiply the input by a matrix and then add a bias vector.

softmaxLayer creates a softmax layer. This layer is very useful for classification problems.

classificationLayer() creates a classification output layer for a neural network. The classification output layer holds the name of the loss function that is used for training the network, the size of the output, and the class labels.

Once all the layers are set then the layers are combined as follow.

layers = [inputLayer middleLayers finalLayers]

Once all the parameters are set then the value of those parameters is fed to the trainNetwork algorithm as follows.

GWI_RCNN= trainNetwork(trainingImages, trainingLabels, layers, opts);

Once all the parameters are set and fed it trainNetwork generates the classification accuracy results along with the progress and time elapsed to provide the results.

3.2 Classification using SVM:

In this case, the learning algorithm has to analyze the data for classification. It works by mapping data into a high-dimensional feature space. The reason for this mapping is to categorize the data points even if data sets can not be separated. A separator between the categories is found and once the separator is found, the data is transformed in such a way that it could be drawn as a hyperplane [41].

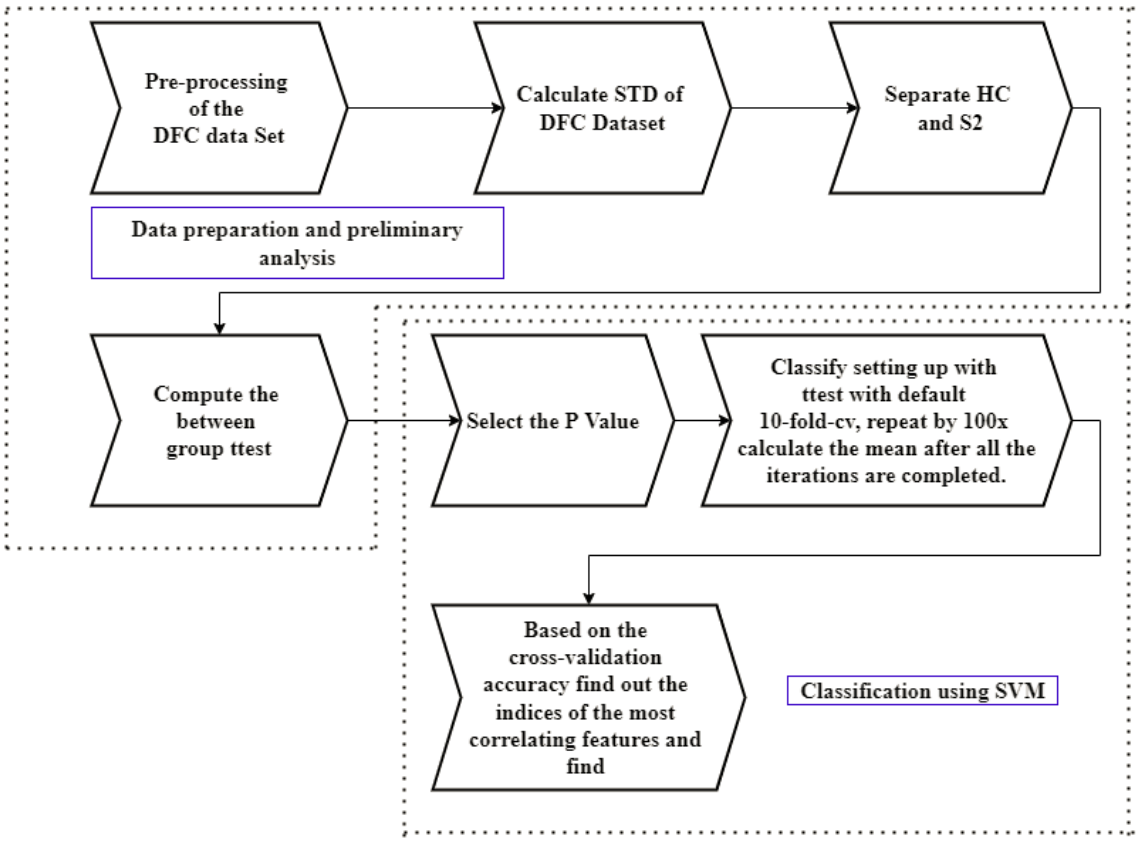

Figure 5: Proposed framework DFC Based Classification of GWI fmri data using SVM.

As GWI DFC data set is 4-D data set, the idea is to first calculate the standard deviation of group zero and group two together. After the standard deviation is calculated, the *ttest2* is performed between the group to reduce the feature, and only those features are selected, which are significant for this classification. Then, *fitcsvm* function of MATLAB is used with the selected input parameters and at the end the mean cross-validation accuracy is calculated and classifying pairs are found.

***Pseudocode*:**

```
all_subject = [group_zero; group_two]
    for i = 1:53
        for u = 1:116
            for v = 1:116
                all_subject_std = squeeze(all_subject(u,v,:,i)
             end
         end
    end

    group_zero_std = all_subject_std(:,:,1 to 30)
    group_zero_std = all_subject_std(:,:,31 to 52)
    t_test = ttest[group_zero_std;group_two_std]
    x_sel = select the feature using test value
    for i 1=100
        svm_x_sel = fitcsvm(x_sel, Y,Standarize, true, KernelFunction,
RBF,…,KernalScale, auto ….)
        cross_validation = crossval(svm_x_sel)
    end
    mean(cross_validation)
```

fitcsvm fit a classification Support Vector Machine (SVM) (model = fitcsvm(data,Y)). It returns an SVM model for data in the input and response. The input contains the predictor variables and Y can be an array of class labels or the name of the variables or formula.

Table 6:

fitcsvm input parameters name and descriptions [40] .

Parameters	**Description**
Standardize	It is a logical scalar and defualt value is set to false. If it has the value true, it standardizes X by centering and dividing columns by their standard deviations. In this case true is selected
KernelFunction	It is defined as function G = KFUN (U, V). The value G is a matrix of size M by N where M and N are the number of rows in U and V. It is a string specifying function the for computing elements of the gram matrix. It can have linear, Gaussian, polynomial or the name of the user-defined function on the MATLAB path. The default value is linear. In this case RBF is selected
KernelScale	It is the scaling factor it can have an auto or positive scalar specifying the scale factor. It selects an appropriate scale factor using a specific procedure. In this case auto has been selected.

CHAPTER IV:

RESULTS

4.1 DFC R-CNN Results:

During this work, several mechanisms were tried to calculate the classification using R-CNN. Results obtained from some of them are explained below, such as, classification utilizing all the features, classification using reduced features (mean and standard deviation), and classification using selective features of AAL ATLAS.

4.1.1 DFC Classification results utilizing all the features:

All the features of the 4-D matrix were utilized to perform the classification. Close to half a million features were there in this case. Group zero and group two data were stored as shown below. Group zero's dimensions are 30×116×116×37 and group two's dimensions are 23×116×116×37, since group zero has 30 subjects,

GroupZero = myROIDFC_GroupZero.mat

GroupTwo = myROIDFC_GroupTwo.mat

After the data were stored in these variables, as per the pseudo-code explained in section 3.1, the training labels were created, and converted into categorical. The reason we convert the label into categorical is that it provides efficient storage capabilities and convenient manipulation of data. After the data labels were created, the options and other parameters for the training algorithm were set and run for a few iterations. During each iteration, cross-validation accuracy was stored in a separate variable. After the n^{th} iteration mean cross-validation accuracy was calculated.

In this architecture we have one image input layer, nine middle layers and five final layers.

Table 7:

Layers description for the first set of parameters while training of the data is on.

Sequence	**Layer**	**Name of the Layer**	**Description During the Training Process**
1	Image Input Layer	Image Input	116×116×37 images with 'zerocenter' normalization
2	Middle Layer	Convolution	64 11×11 convolutions with stride [1 1] and padding [3 3 3 3]
3	Middle Layer	ReLU	ReLU
4	Middle Layer	Max Pooling	3×3 max pooling with stride [2 2] and padding [0 0 0 0]
5	Middle Layer	Convolution	64 11×11 convolutions with stride [1 1] and padding [3 3 3 3]
6	Middle Layer	ReLU	ReLU
7	Middle Layer	Max Pooling	3×3 max pooling with stride [2 2] and padding [0 0 0 0]
8	Middle Layer	Convolution	128 11×11 convolutions with stride [1 1] and padding [2 2 2 2]
9	Middle Layer	ReLU	ReLU
10	Middle Layer	Max Pooling	3×3 max pooling with stride [2 2] and padding [0 0 0 0]
11	Final Layer	Fully Connected	64 fully connected layer
12	Final Layer	ReLU	ReLU
13	Final Layer	Fully Connected	2 fully connected layer
14	Final Layer	Softmax	softmax
15	Final Layer	Classification Output	crossentropyex

Training progression for the first set of parameters stated in section 3.1 table 3 is explained below. The first iteration results are:

Table 8:

First iteration training progression with validation accuracy, mini batch loss base learning rate, iterations, epoch, and time elapsed.

Epoch	Iteration	Time Elapsed (hh:mm:ss)	Mini-batch Accuracy	Validation Accuracy	Mini-batch Loss	Validation Loss	Base Learning Rate
1	1	00:00:09	66.67%	57.69%	0.6923	0.6894	0.0100
5	15	00:00:58	100.00%	50.00%	0.1499	1.8633	0.0100
10	30	00:01:56	88.89%	65.38%	0.2272	4.0254	0.0010
15	45	00:02:45	100.00%	61.54%	0.0366	3.5159	0.0010
17	50	00:03:01	88.89%		0.1017		1.0000e-04
20	60	00:03:37	100.00%	57.69%	0.0071	4.5683	1.0000e-04

In this case, validation accuracy settled down around 0.5769(57.69%) and validation loss was close to 4.6. It took around 3 minutes and 40 seconds to complete the first iteration. The figure below shows the MATLAB training progression with details.

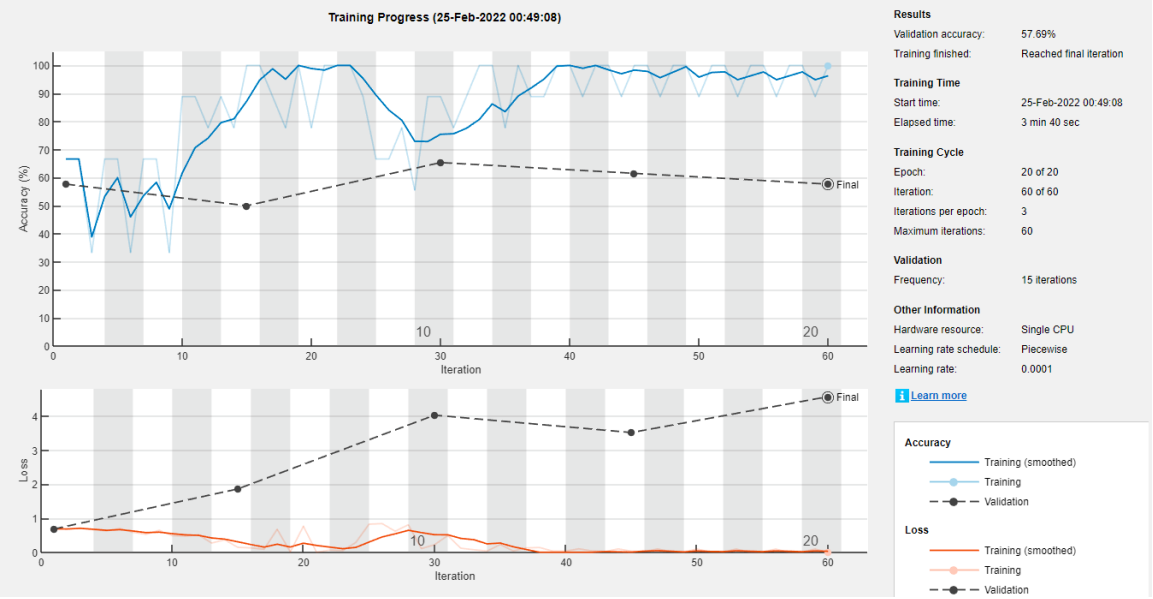

Figure 6: First iteration training progression on MATLAB output window.

Second iteration results are explained below.

Table 9:

Second iteration training progression with validation accuracy, mini-batch loss base learning rate, iterations, epoch, and time elapsed.

Epoch	Iteration	Time Elapsed (hh:mm:ss)	Mini-batch Accuracy	Validation Accuracy	Mini-batch Loss	Validation Loss	Base Learning Rate
1	1	00:00:11	66.67%	46.15%	0.6929	0.7004	0.0100
15	15	00:01:07	100.00%	38.46%	2.0168e-05	7.0552	0.0010
20	20	00:01:25	100.00%	38.46%	-0.0000e+00	8.4737	1.0000e-04

In the second iteration, case validation accuracy settled down around 0.3846(38.46%) and validation loss was close to 8.47. It took around 1 minute and 27 seconds to complete the second iteration. The figure below shows the MATLAB training progression with details.

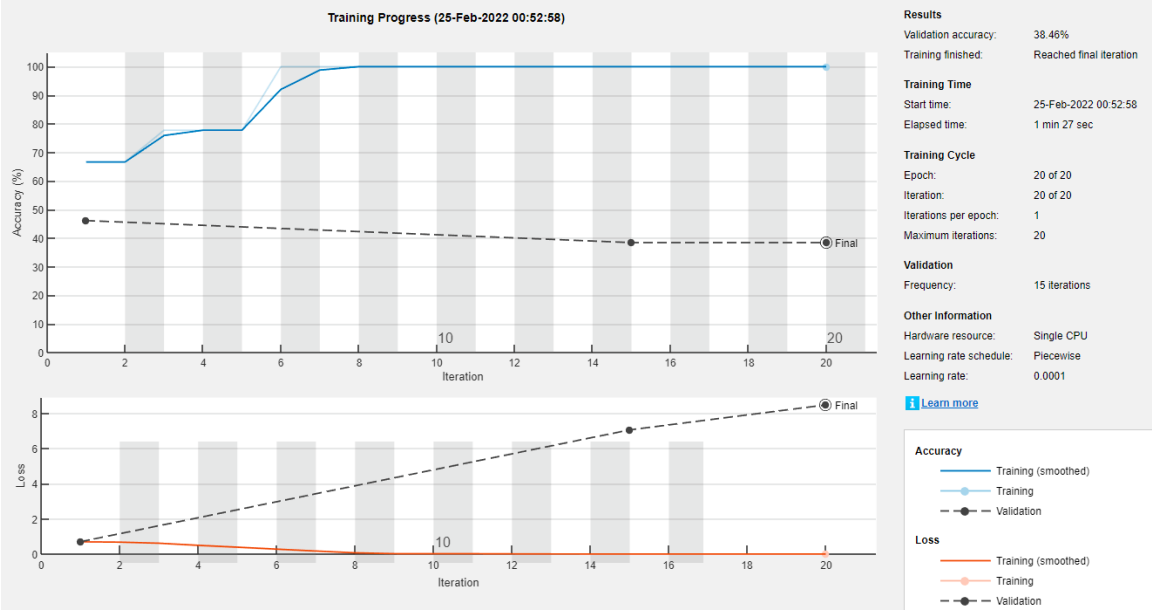

Figure 7: Second iteration training progression on MATLAB output window.

The third iteration results are explained below.

Table 10:

Third iteration training progression with validation accuracy, mini-batch loss base learning rate, iterations, epoch, and time elapsed.

Epoch	Iteration	Time Elapsed (hh:mm:ss)	Mini-batch Accuracy	Validation Accuracy	Mini-batch Loss	Validation Loss	Base Learning Rate
1	1	00:00:12	28.57%	71.43%	0.6937	0.6906	0.0100
15	15	00:01:07	100.00%	57.14%	0.0003	2.0620	0.0010
20	20	00:01:23	100.00%	42.86%	4.9387e-07	3.3903	1.0000e-04

In the third iteration, case-validation accuracy started at approximately 71%. However, it settled down at around 43% and validation loss was close to 3.4. It took around 1 minute and 23 seconds to complete the third iteration. The figure below shows the MATLAB training progression with details.

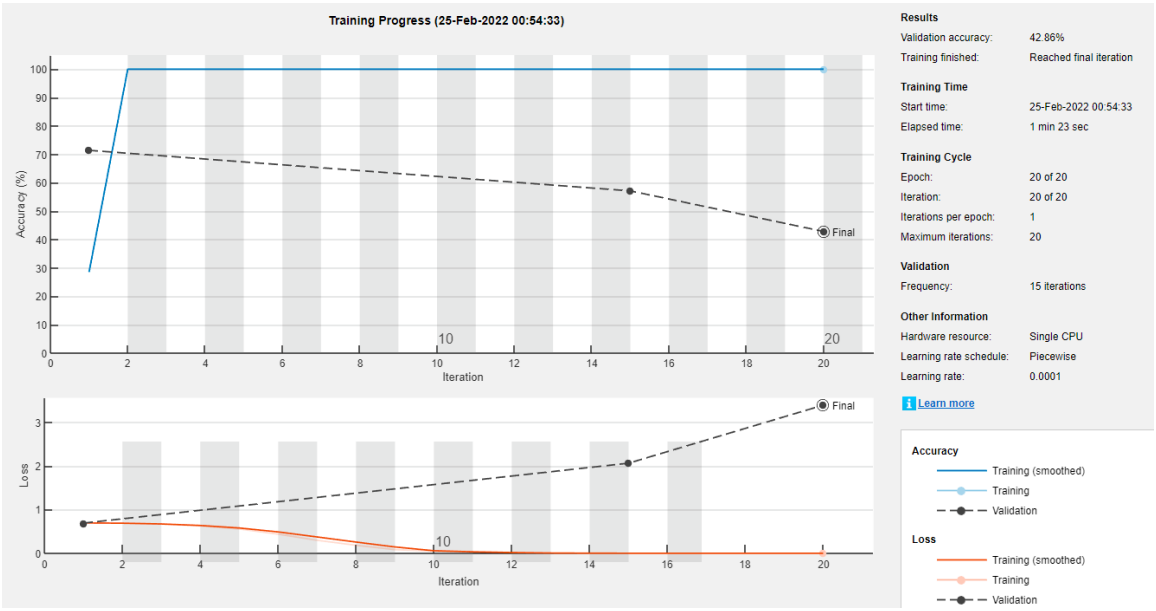

Figure 8: Third iteration training progression on MATLAB output window.

The final iteration results are explained below.

Table 11:

Fourth iteration training progression with validation accuracy, mini-batch loss base learning rate, iterations, epoch, and time elapsed.

Epoch	Iteration	Time Elapsed (hh:mm:ss)	Mini-batch Accuracy	Validation Accuracy	Mini-batch Loss	Validation Loss	Base Learning Rate
1	1	00:00:30	25.00%	66.67%	0.6944	0.6899	0.0100
15	15	00:01:12	100.00%	66.67%	-0.0000e+00	5.3141	0.0010
20	20	00:01:27	100.00%	66.67%	-0.0000e+00	5.3141	1.0000e-04

In the fourth and final iteration, case validation accuracy started at approximately 66.67% and settled down at around 66.67% and validation loss was close to 5.3. It took around 1 minute and 27 seconds to complete this iteration. The figure below shows the MATLAB training progression with details.

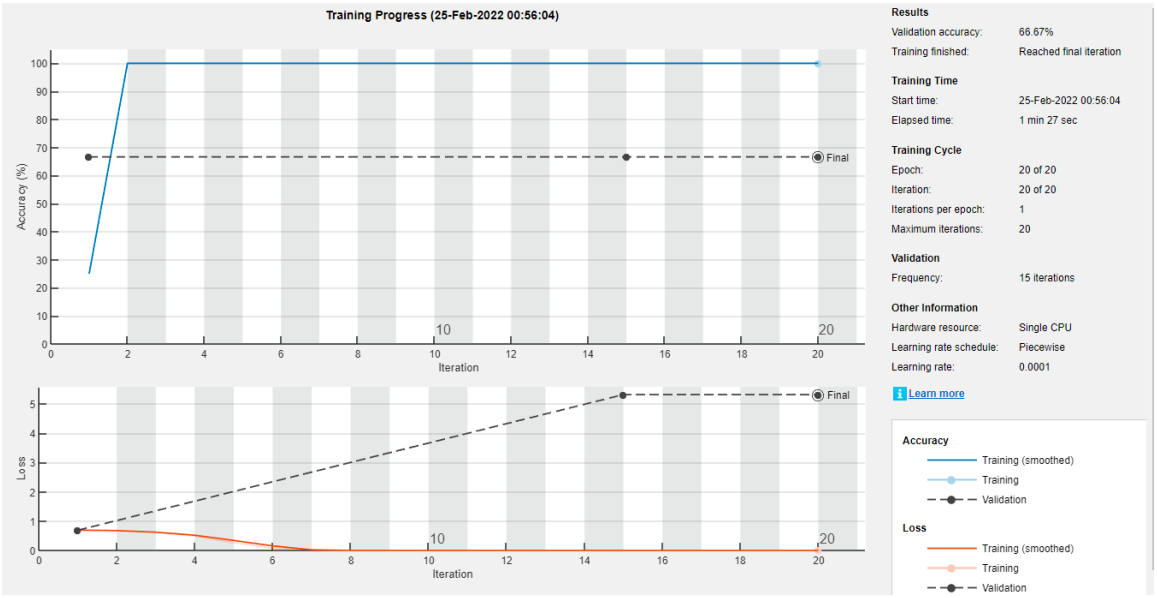

Figure 9: Fourth iteration training progression on MATLAB output window.

After all the iterations were completed, the mean cross-validation accuracy was calculated as 0.5142(51.42%) and a similar approach was taken to execute it for the parameter set two and three. Comparison of all the three parameter-sets (Table 3, 4 and 5) results are explained below.

Table 12:

Comparison of Mean Cross- Validation accuracy among different parameter sets.

Parameter Sets	No of Iteration	Mean CV Accuracy
1	4	0.5142
2	4	0.4785
3	3	0.4963

For parameter set 3, we obtained the cross-validation accuracy of 0.4963(49.63%). The above table depicts that parameter sets do not vary the results much and the model settles down around 50% of accuracy.

4.1.2 DFC Classification results utilizing mean and standard deviation:

In this case mean and standard deviation were calculated across the DFC windows to reduce the number of features, but the results did not improve and settled down to 50%. Here, three different parameter sets were used to calculate the classification accuracy. In the first set of parameters, mean cross-validation accuracy came to 0.49(~49%). It was run for four iterations. In the first iteration, cross-validation accuracy was calculated as 0.42; in the second iteration, it came to 0.46; in the third iteration, the mean CV accuracy was 0.538 and in the fourth iteration, it was 0.538, averaging overall into 0.49.

Training progresses in each iteration is explained below.

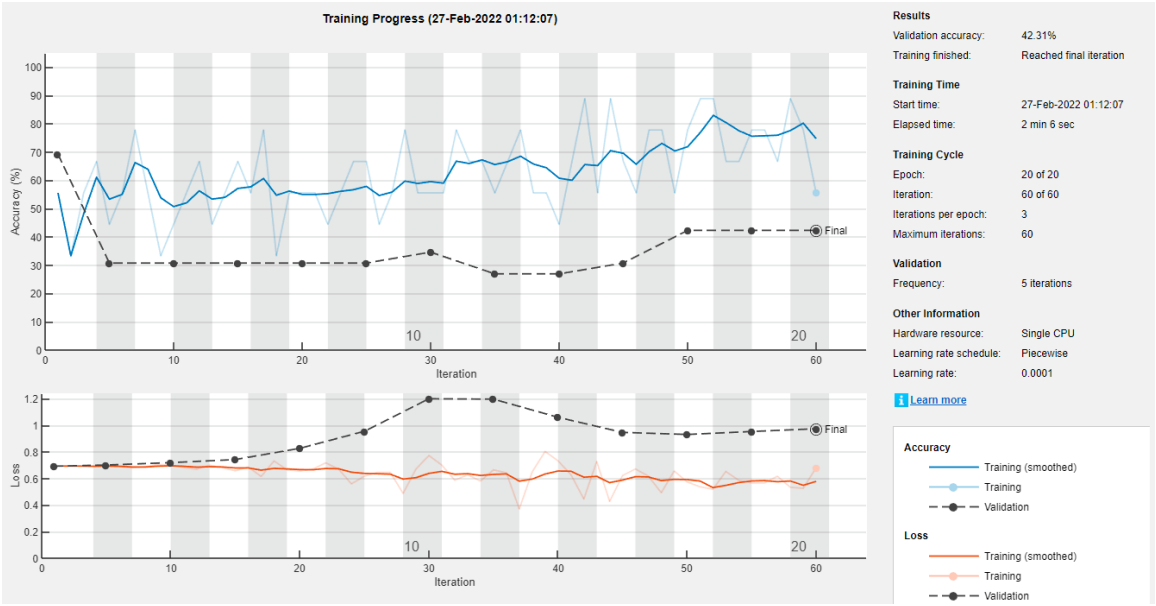

Figure 10: First iteration training progression on MATLAB output window for classification utilizing mean and standard deviation.

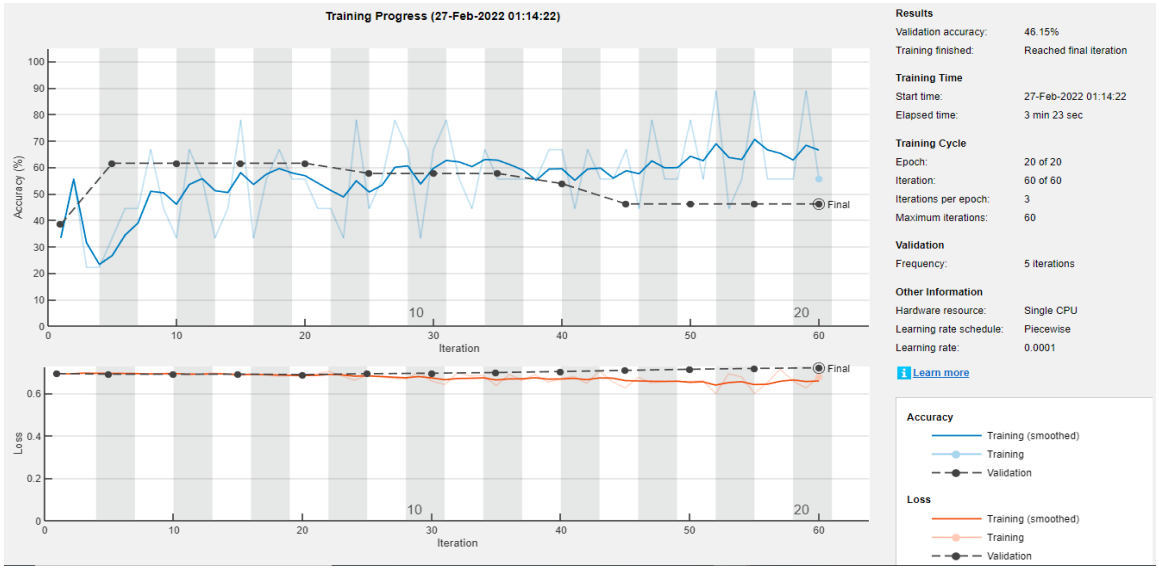

Figure 11: Second iteration training progression on MATLAB output window for classification utilizing mean and standard deviation.

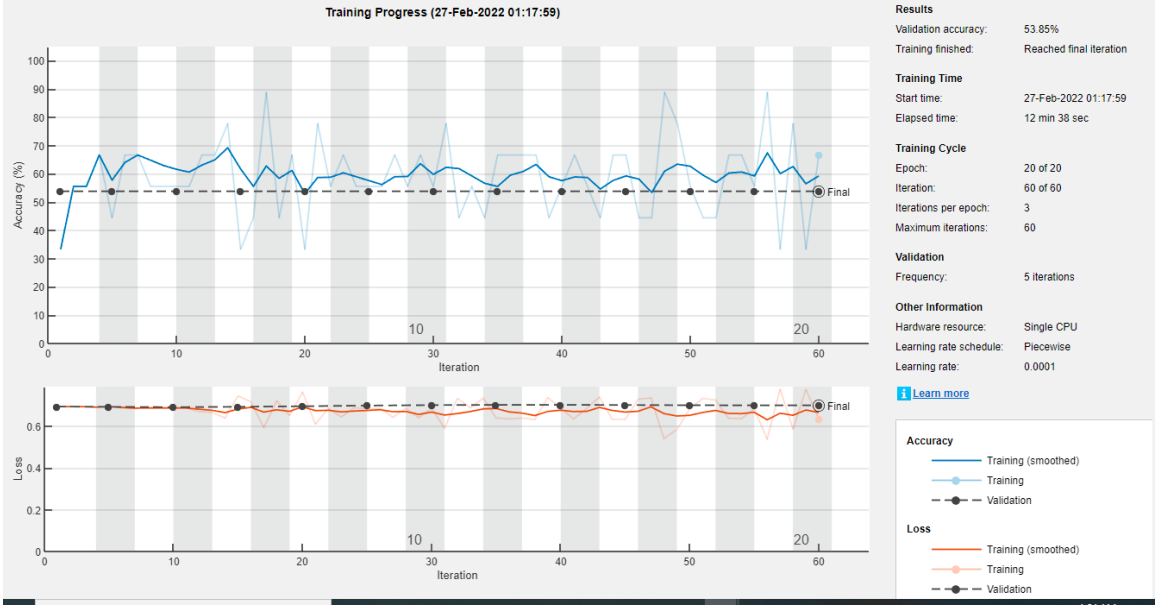

Figure 12: Third iteration training progression on MATLAB output window for classification utilizing mean and standard deviation.

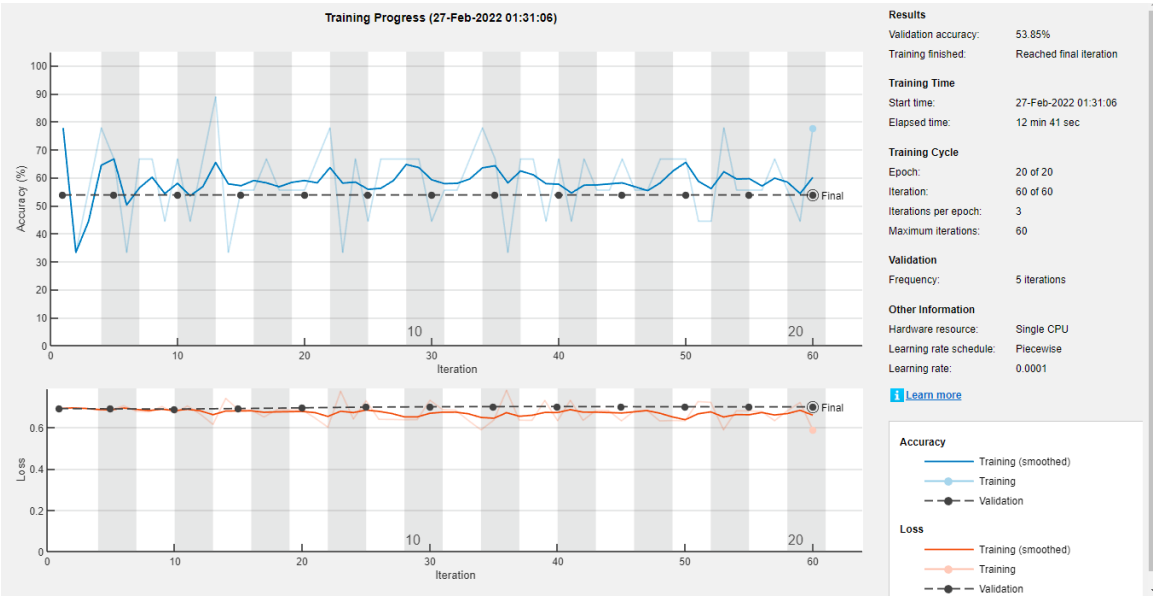

Figure 13: Fourth iteration training progression on MATLAB output window for classification utilizing mean and standard deviation.

Classification using mean and standard deviation took significantly more time to train than utilizing all the features. For the same set of parameters, the latter took 20 minutes more than the former, and the results did not change much.

After running through the first set of parameters, it is important to check with the remaining two to see how results vary. Results from all three sets of parameters (Tables 3, 4, and 5) can be found below.

Table 13:

Comparison of Mean Cross- Validation accuracy among different parameter sets using mean and standard deviation across one dimension.

Parameter Sets	No of Iteration	Mean CV Accuracy
1	4	0.49
2	4	0.44
3	4	0.49

4.1.3 DFC Classification results utilizing selective features (selective brain regions of AAL ATLAS):

Selective features were used in this case to check the results. The idea was to calculate the classification accuracy using selective brain region. Here, the selective brain regions for all the subjects were utilized to calculate the accuracy. Brain regions selected to calculate classification accuracy are listed below in the tabular form (table 15) [36]. These regions were tried for three different parameter sets, each for four iterations, but the results remained close to 50%. Consolidated results for each parameter set (Tables 3, 4, and 5) are stated below.

Table 14:

Comparison of Mean Cross- Validation accuracy among different parameter sets using selective brain region.

Parameter Sets	No of Iteration	Mean CV Accuracy
1	4	0.49
2	4	0.51
3	4	0.4808

Table 15*:*

List of selected brain regions used for calculating classification accuracy.

Brain Region Label	Brain Region Name
19	Supp_Motor_Area_L 2401
20	Supp_Motor_Area_R 2402
47	Lingual_L 5021
48	Lingual_R 5022
81	Temporal_Sup_L 8111
82	Temporal_Sup_R 8112
85	Temporal_Mid_L 8201
86	Temporal_Mid_R 8202

4.2 FC R-CNN Results:

To conclude on the results obtained in the previous section, it was important to perform a similar classification analysis on the FC data set. During this work, classification accuracies were calculated using R-CNN techniques. First, the accuracies were calculated using all the features. After that, the mean and standard deviation were calculated across one region dimension and were applied to the R-CNN techniques to find the accuracies; and lastly, we utilized the selective brain regions listed in table Table 16. During this process, we calculated the accuracies utilizing the parameter sets listed in Table 3, 4 and 5.

4.2.1 FC Classification results utilizing all the features:

FC data set is a 3D matrix (number of object vs number of brain regions vs number of brain regions). During this exercise, we utilized all the features and trained the network with same algorithms discussed in DFC with same parameter set.

Table 16:

Comparison of Mean Cross- Validation accuracy among different parameter sets utilizing all features for FC data set.

Parameter Sets	No of Iteration	Mean CV Accuracy for FC Data Set
1	4	0.4592
2	4	0.4341
3	4	0.5408

4.2.2 FC Classification results utilizing mean and standard deviation:

Like section 4.1.2, the mean and standard deviation across the 'brain region' were calculated, and the classification cross-validation accuracy and results were obtained for each parameter sets are shown below.

Table 17:

Comparison of Mean Cross-Validation accuracy among different parameter sets utilizing mean and standard deviation for FC data set.

Parameter Sets	No of Iteration	Mean CV Accuracy for FC Data Set
1	4	0.6062
2	3	0.4002
3	4	0.5215

4.2.3 FC Classification results utilizing selected brain region features using AAL ATLAS:

As mentioned earlier, in this case, selective brains regions were taken which were selected based on the previous study [36]. During this, there were handful of brain regions (table 15).

Table 18:

Comparison of Mean Cross-Validation accuracy among different parameter sets utilizing selective features of FC data set.

Parameter Sets	No of Iteration	Mean CV Accuracy for FC Data Set
1	3	0.5385
2	3	5256
3	4	0.50

4.3 Comparative study of DFC and FC using R-CNN:

The idea of this study was to draw some conclusions between DFC and FC using R-CNN. However, results in both cases were found around 50 percent. Even after increasing the number of iterations to 100, classification accuracy was close to 50%. If we compare the Table 12 and Table 16, the results are not very distinguishable. Similarly, comparing tables 13 and 17 or 14 and 18 we see the minimal differences in the results. Comprehensively, we cannot draw any conclusion based on the results obtained using R-CNN on FC and DFC. However, the expectation from DFC based classification was to provide the better results, as it has significantly more features compared to FC.

4.4 SVM-based classification results of DFC data set:

During this research work, after obtaining the results using R-CNN, we implemented the same data set to SVM using fitcsvm. Results obtained from some of them are explained below. We used *ttest2* to find out the suitable pairs to be used for classification.

4.4.1 SVM-based classification results of DFC data set for different P Values:

During this exercise, we utilized AAL ATLAS based DFC group zero and group two data sets.

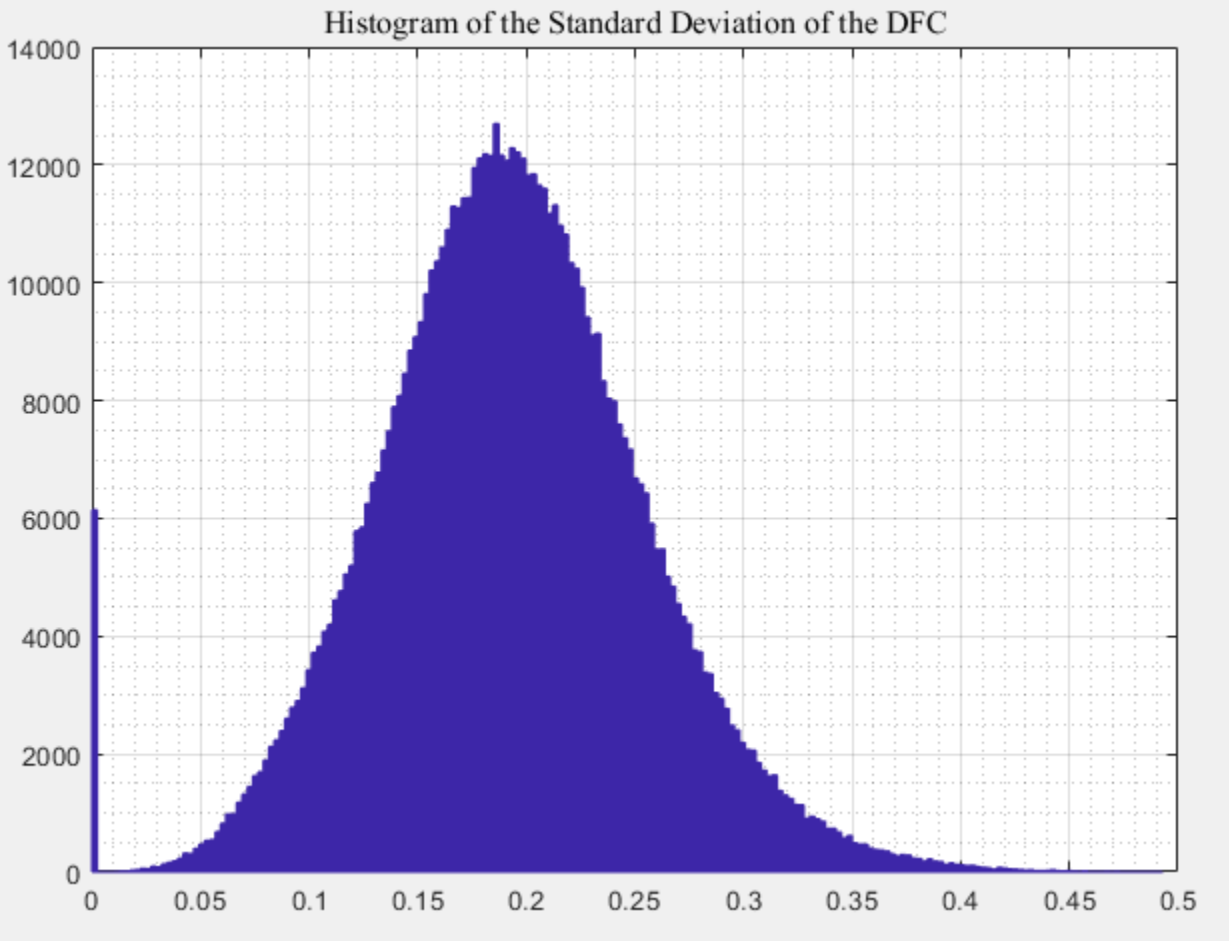

Figure 14: Histogram of the standard deviation of the DFC (Combining HC and S2).

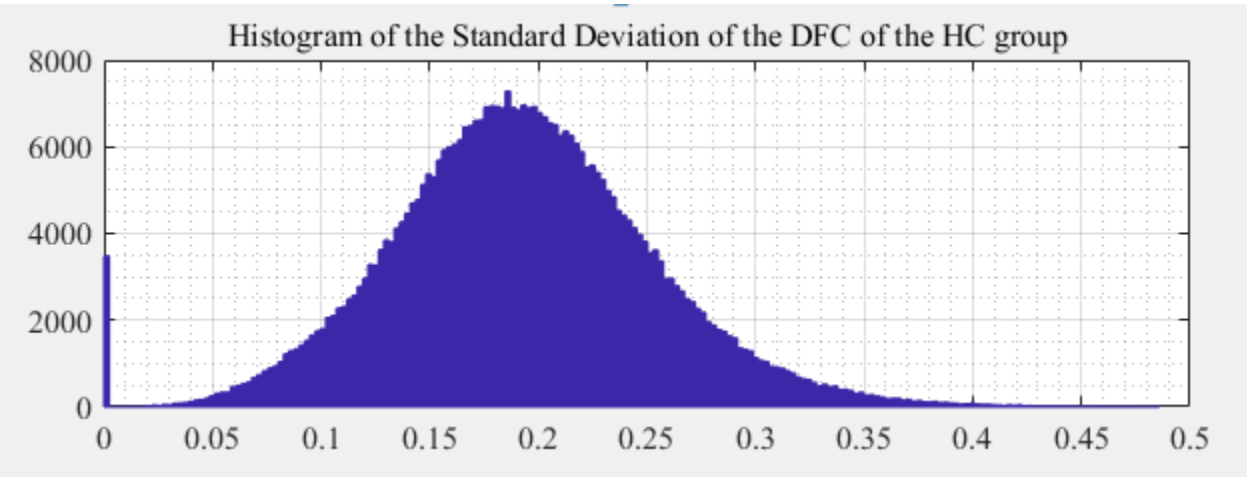

Figure 15: Histogram of the standard deviation of the DFC HC group.

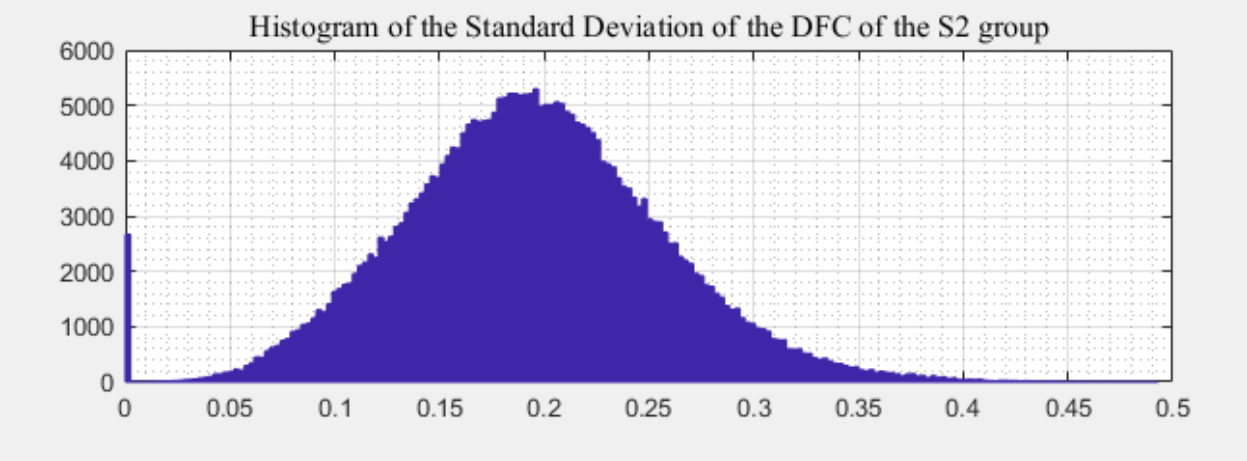

Figure 16: Histogram of the standard deviation of the DFC S2 group.

Histograms were obtained just to check the distribution of the standard deviations among all the features. After this, we calculated ttest2 utilizing below formula.

[h p c stats] = ttest2(__) [40].

In the above formula, h stands for hypothesis, and it has two values, 0 or 1. If 0, it indicates that the null hypothesis at the alpha significance level cannot be rejected at 5% and if *h* has the value of 1, the null hypothesis at the alpha significance level can be rejected at 5%.

p in the above formula stands for probability of observing a test statistic as extreme. It ranges values between 0 and 1.

c stands for confidence intervals for the difference in population.

Test statistics for the two-sample *t*-test returned as a structure containing the following:

tstat — Value of the test statistic.

df — Degrees of freedom of the test.

sd — Pooled estimate of the population standard deviation (for the equal variance case) or a vector containing the unpooled estimates of the population standard deviations (for the unequal variance case) [40].

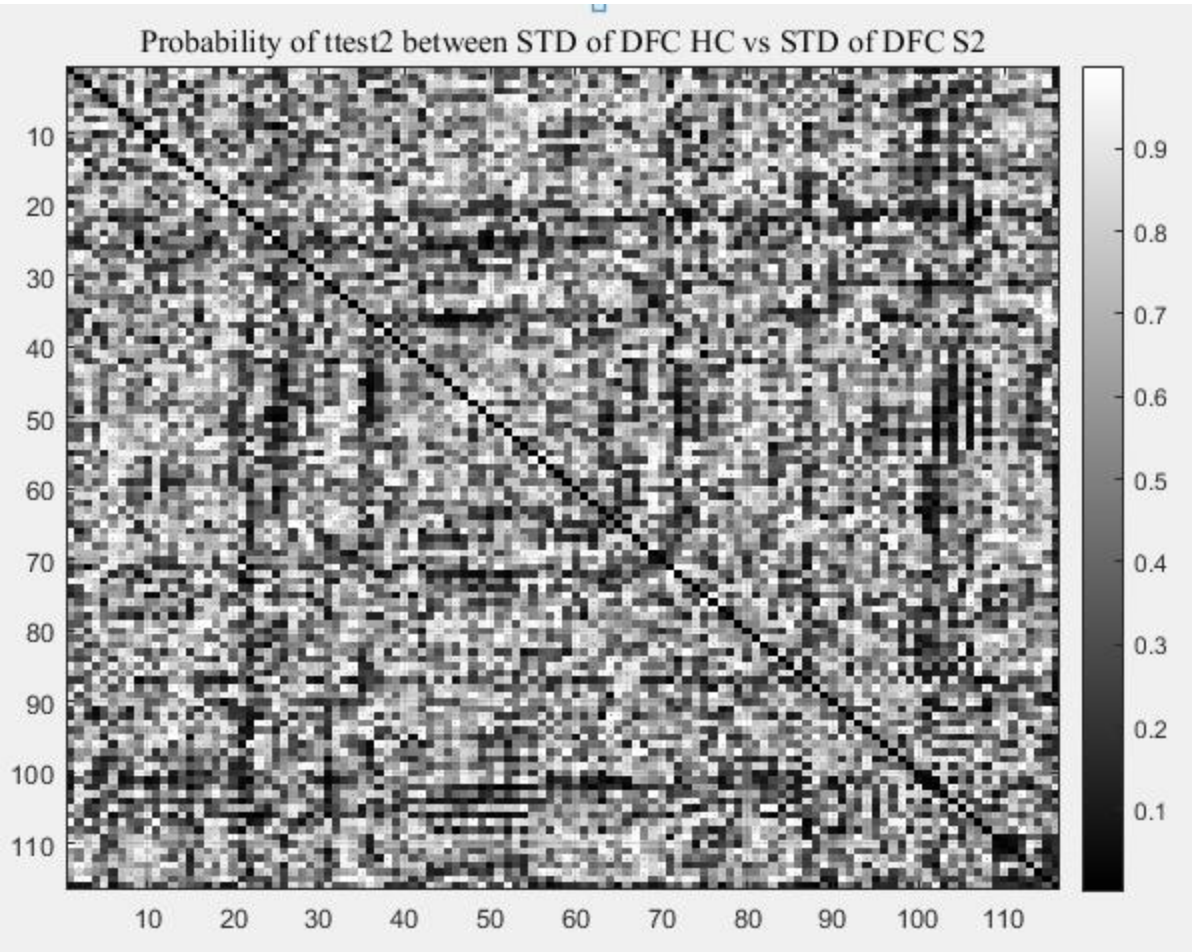

Figure 17: Probability of ttest2 between STD of DFC HC vs STD of DFC S2.

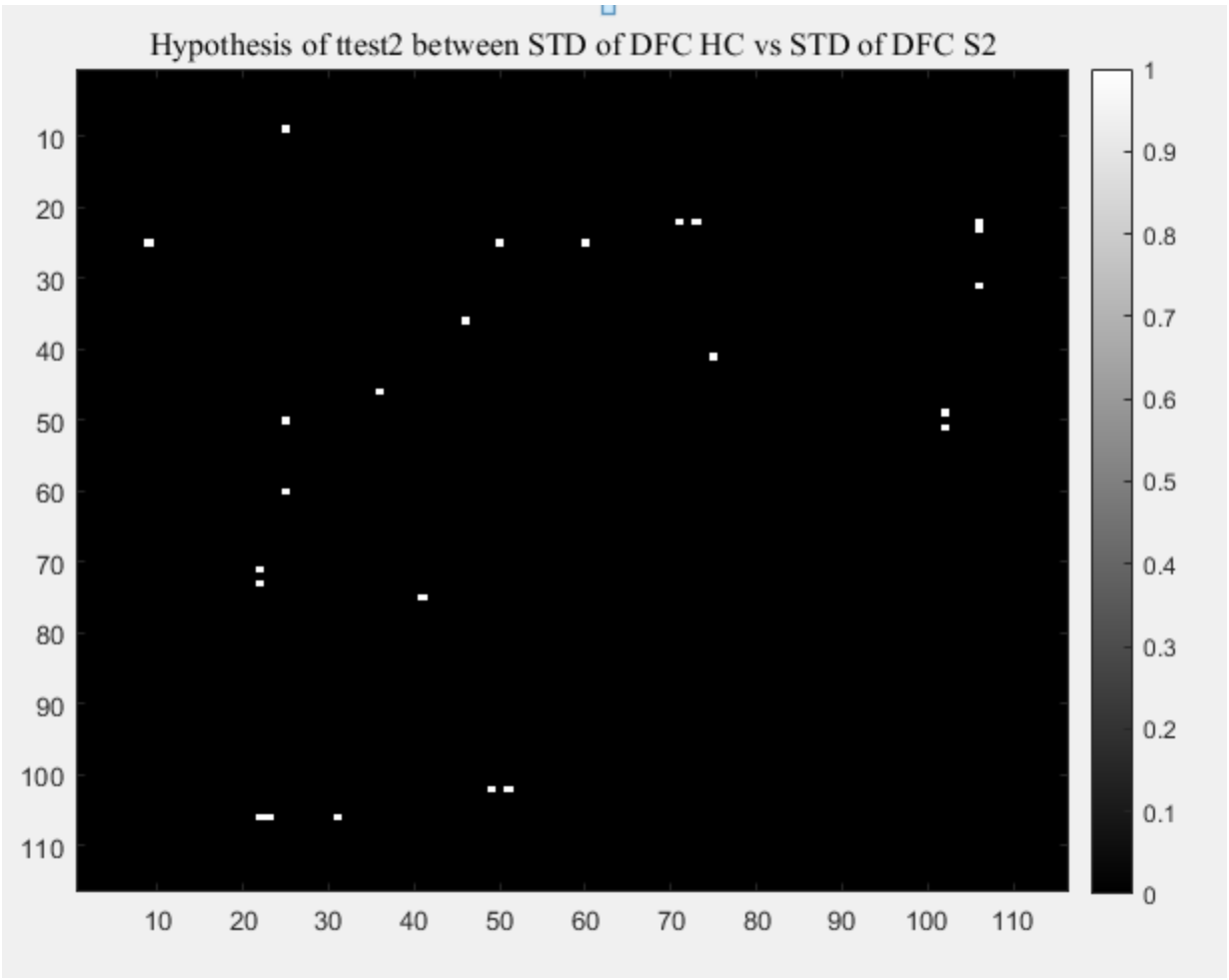

Figure 18: Hypothesis of ttest2 between STD of DFC HC vs STD of DFC S2.

Once ttest2 is performed on the data set, it provides the *p, h, c,* and *stats* values. The value obtained for *p* is 116X116 double and each element's value is greater than zero and less than 1(except the diagonal element). Similarly, *h* is also a 116X116 double. *c* is a 116X116X2 double value and as mentioned above *stats* has three components *tstat, df,* and *sd. tstat* and *df* are 116X116 double and *sd* are 116X116X2 double. Based on the results obtained above, first we preformed classification using default 10-fold-cv and repeated it by 100x and took the average. Mean cross-validation loss utilizing all the features came around 0.3543 which is ~ 35% cross-validation loss and ~65% classification accuracy. So, with SVM method, results improved, but no significant differences were seen if all the features were utilized in both SVM and R-CNN.

After this, we utilized the *p* value obtained during ttset2 and checked how the results were coming along.

4.4.1.1 SVM-based classification for DFC data set for P < 0.001:

Utilizing ttest2 results is a way of reducing the features which is not relevant for our exercise. So, only those features were selected, whose probability was less than 0.001. With this probability, only one pair existed. This pair was identified as number 25 (Frontal_Med_Orb_L 2611) and 50 (Occipital_Sup_R 5102) of brain region.

In this case also, classification was calculated based on STD DFC with default 10-fold-cv and repeated by 100x and mean cross-validation loss of 0.3543 were obtained. It means, classification accuracy of 64.57% was obtained.

4.4.1.2 SVM-based classification for DFC data set for P < 0.05:

We started with the minimum *p* value (<0.001) where only one pair was found, so we determined to increase the *p* value and calculated the cross-validation accuracy for several *p* values and listed down in Table 19. With *p* value <0.05, 113 pairs were found. Classification was calculated based on STD DFC with default 10-fold-cv and repeated by 100x and mean cross-validation loss of 0.0191 were obtained, which means, classification accuracy was ~ 98 percent. In all the ten cases of PDFC value, one common pair was obtained as shown in figure 19.

Table 19:

SVM AAL ATLAS Based Classification accuracy, Mean K fold cross-validation loss obtained for corresponding P DFC value.

Maximum P DFC	Mean K fold Loss	Classification Accuracy	Number of Pairs
0.001	0.3543	0.6457	2/2=1
0.002	0.3934	0.6066	4/2=2
0.005	0.1792	0.8208	8/2=4
0.01	0.1932	0.8068	24/2=12
0.02	0.0628	0.9372	64/2=32
0.03	0.06	0.94	124/2=62
0.04	0.0358	0.9642	174/2=87
0.05	0.0191	0.9809	226/2=113
0.06	0.0494	0.9506	298/2=149
0.1	0.0492	0.9508	610/2=305

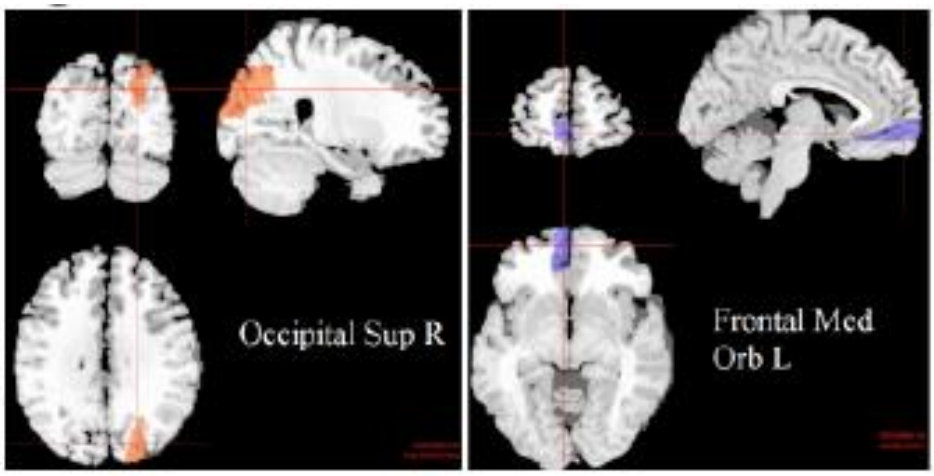

Figure 19: The two AAL regions (left: Right Superior Occipital Gyrus, marked with red, and right: Left Medial Orbital Superior Frontal Gyrus, marked with blue) constituting the region-pair with the most discriminating power across the two groups GWI vs NC, with stdDFC. The average standard deviation of the temporal-evolution/dynamics of the DFC (stdDFC) between these two regions was significantly lower in GWI than in NC ($p<0.001$). The classification accuracy of was 98% (52/53 or missing only one participant) [42].

4.5 SVM-based classification results of FC data set:

After obtaining the results using R-CNN, we implemented the same data set to SVM using fitcsvm. Results obtained from some of them are explained below. In this process we used *ttest2* to find out the suitable pairs to be used for classification.

4.5.1 SVM-based classification results of FC data set for different P values:

During this exercise we utilized AAL ATLAS based FC group zero and group two data set.

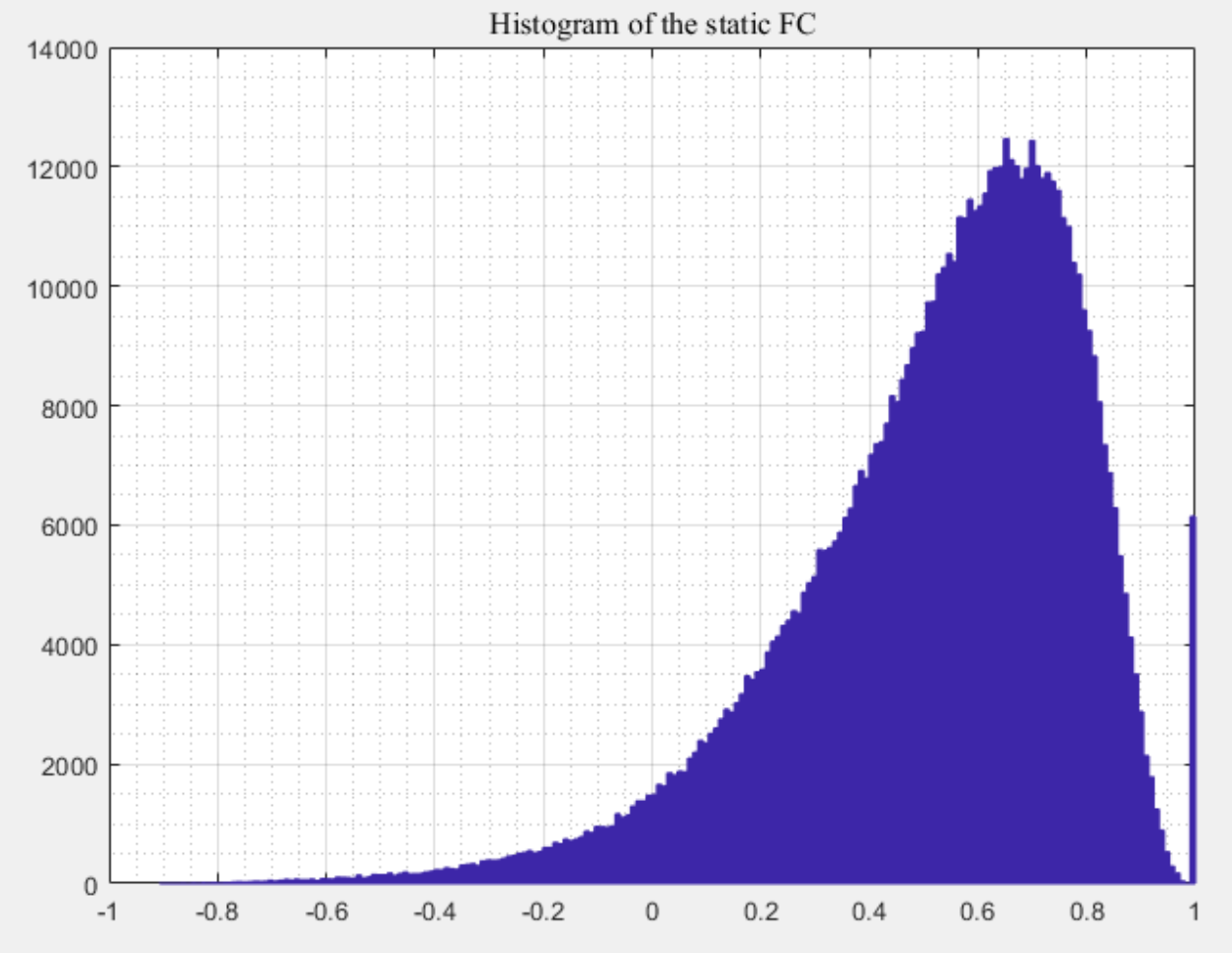

Figure 20: Histogram of the of the FC (Combining HC and S2).

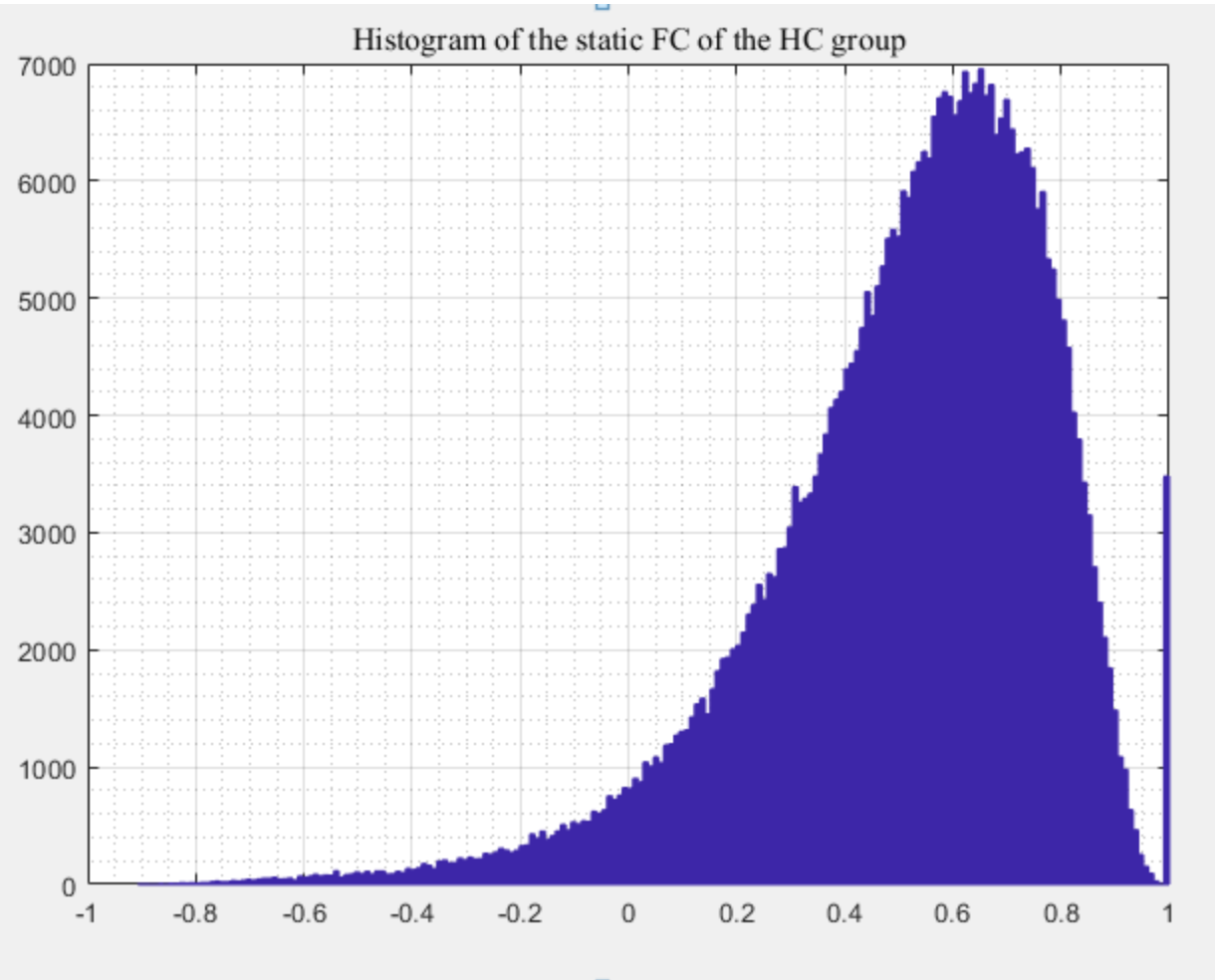

Figure 21: Histogram of the standard deviation of the FC HC group.

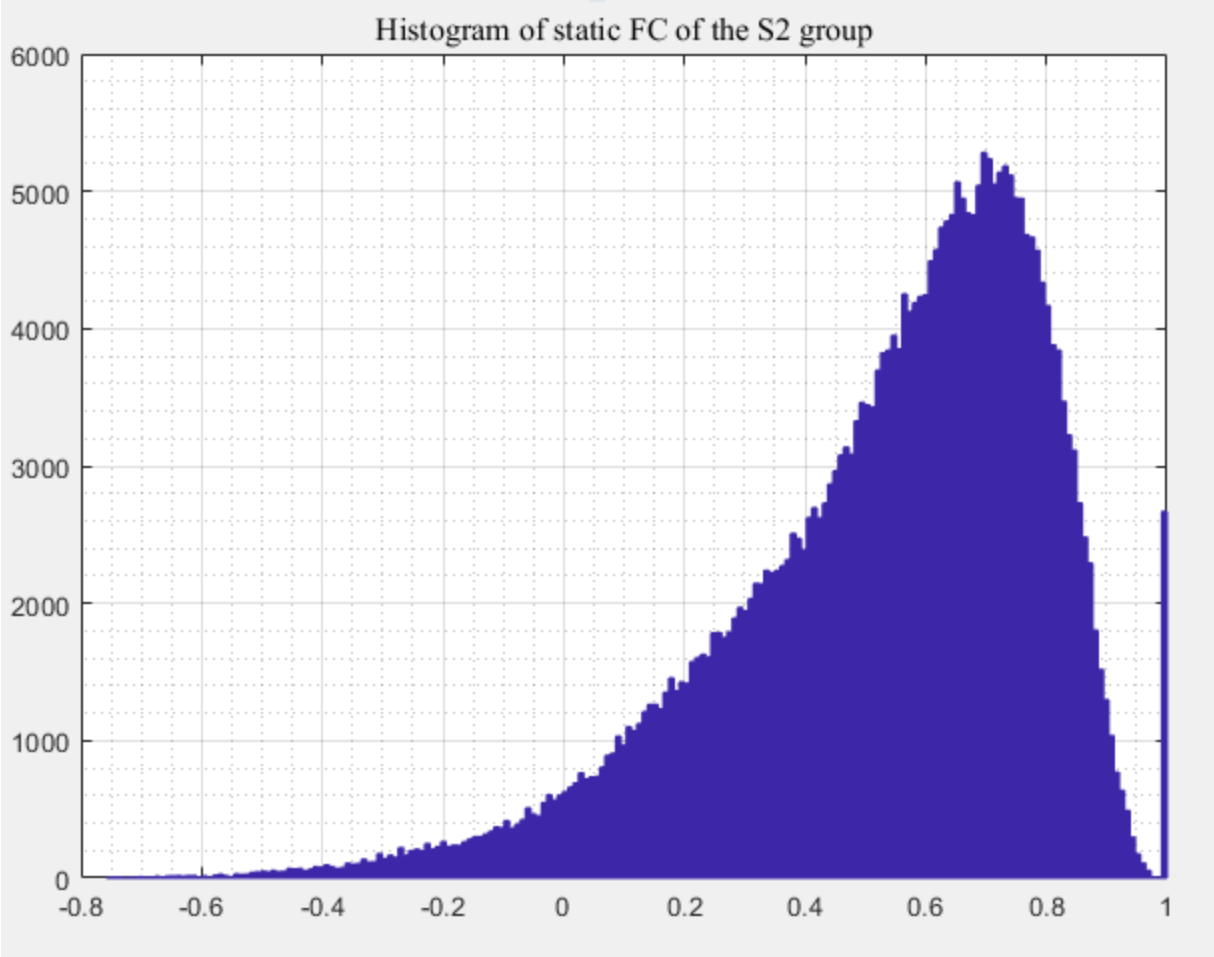

Figure 22: Histogram of the standard deviation of the FC S2 group.

Histograms were obtained just to check the distribution of the standard deviations among all the features. After this we calculated the ttest2 utilizing formula explained in section 4.4.1.

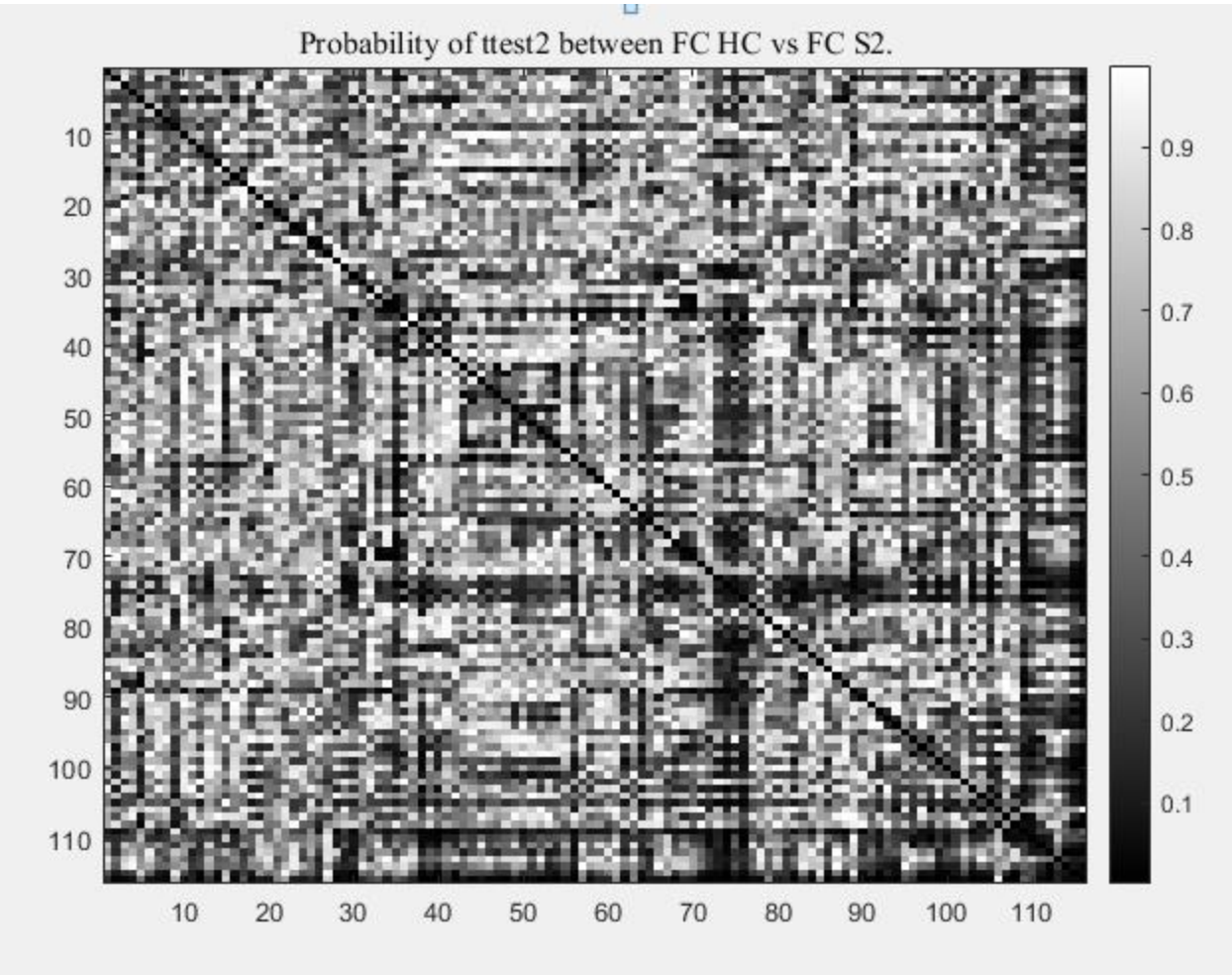

Figure 23: Probability of ttest2 between FC HC vs FC S2.

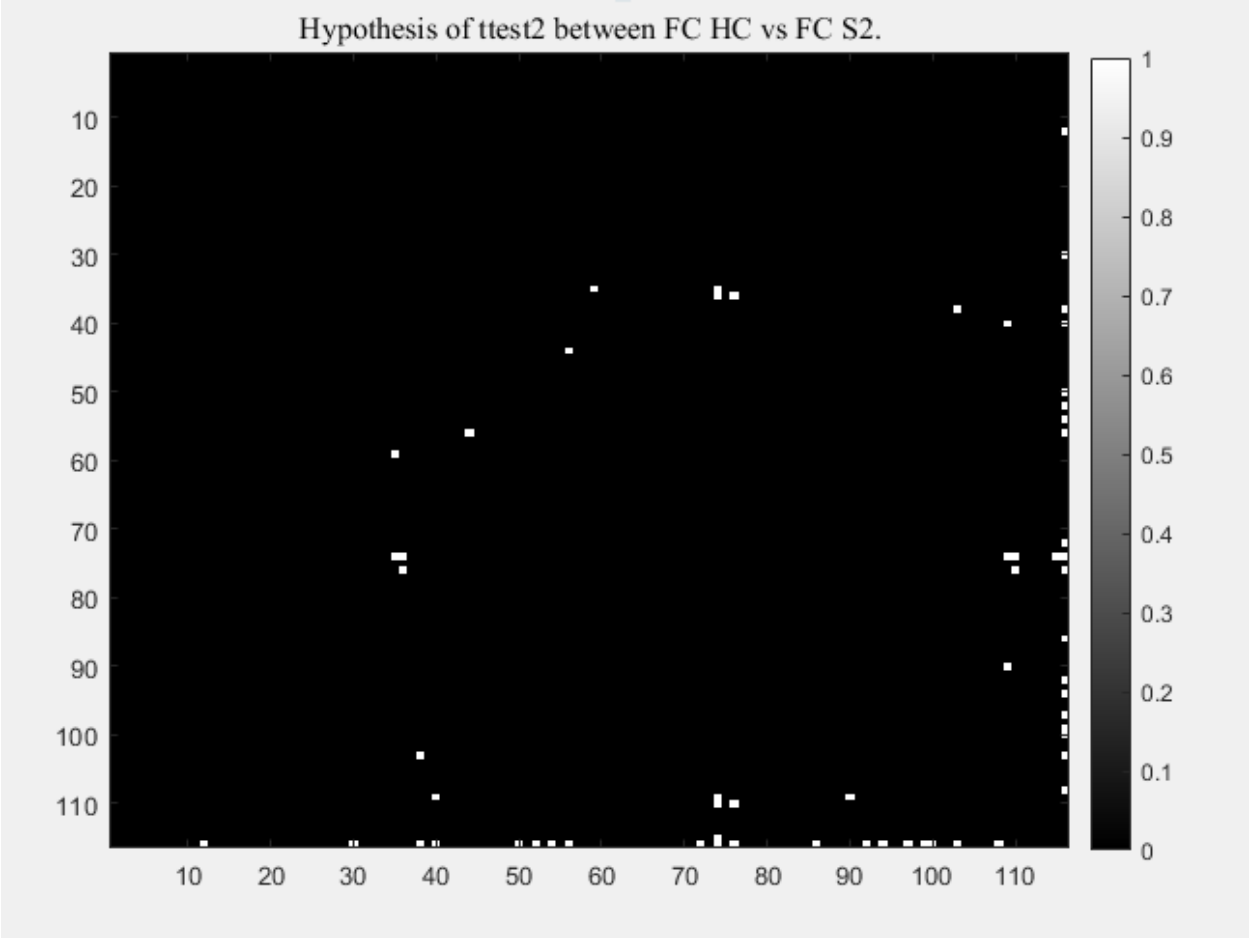

Figure 24: Hypothesis of ttest2 between FC HC vs FC S2.

When *ttest2* was performed on the FC data set, it provided the *p, h, c* and *stat* values. Dimensions of *p, h, c* and *stat* remained the same as in section 4.4.1, however, values to each component varied from what we obtained in DFC. With both FC and DFC data set, the dimension of *p* obtained was 116X116, *h* 116X116 and *c* 116X116X2.

stats has three components: *tstat, df* and *sd. tstat* and *df* are 116X116 double and *sd* is 116X116X2 double. Based on the results obtained above, first we preformed classification using default 10-fold-cv and repeated it by 100x and took the average. Mean cross-validation loss utilizing all the features came around 0.3319 which was ~33% cross-validation loss and ~67% classification accuracy. So, results improved with SVM, but no significant improvement were seen utilizing all the features in both SVM and R-CNN. After this we utilized the *p* value obtained during *ttset2* and checked how the results were coming along.

4.5.1.1 SVM-based classification for FC data set for P < 0.001:

Utilizing ttest2 results is a way of reducing the features which is not relevant for our exercise. So, in this case only those features were selected whose probability was less than 0.001. With this probability, only one pair existed. This pair was identified as number 74 (Putamen_R 7012) and 116 (Vermis_10 9170) of brain region.

Classification was calculated based on FC data with default 10-fold-cv and repeated by 100x and mean cross-validation loss of 0.3319 was obtained. This means classification accuracy of 66.81% was found.

4.5.1.2 SVM-based classification for FC data set for P < 0.05:

We started with the minimum *p* value (<0.001) where we found only one pair, so we determined to increase the *p* value and calculated the cross-validation accuracy for several *p* value and listed down in Table 20. With *p* value <0.05, 234 pairs were found. Classification was calculated based on FC with default 10-fold-cv and repeated by 100x and mean cross-validation loss of 0.3174 was obtained that means classification accuracy was ~ 68 percent.

With FC data set ten different *p* value were tried (listed in Table 20). With *p* value < 0.005, best result of ~72 percent of classification accuracy was found. In all the ten cases, only one pair was common which was identified as number 74 (Putamen_R 7012) and 116 (Vermis_10 9170) of brain region.

Table 20:

SVM AAL ATLAS based classification accuracy, Mean K fold cross-validation loss obtained for corresponding P FC value.

Maximum P FC	Mean K fold Loss	Classification Accuracy	Number of Pairs
0.001	0.3319	0.6681	2/2=1
0.002	0.3108	0.6892	10/2=5
0.005	0.2764	0.7236	26/2=13
0.01	0.3026	0.6974	62/2=31
0.02	0.2885	0.7115	168/2=84
0.03	0.2962	0.7038	262/2=131
0.04	0.3055	0.6945	360/2=180
0.05	0.3174	0.6826	468/2=234
0.06	0.3268	0.6732	560/2=280
0.1	0.3423	0.6577	960/2 = 480

4.6. Some Important Brain Region Pair Obtained:

P DFC less than 0.005 resulted into four brain region pairs. Pair one was ‘Superior frontal gyrus, medial orbital’ and ‘Superior occipital gyrus’. Pair two consisted of ‘Superior frontal gyrus, medial orbital’ and ‘Superior parietal gyrus’. Pair three consisted of ‘Olfactory cortex' and ‘Caudate nucleus’. Pair four consisted of ‘Olfactory cortex’ and ‘Lenticular nucleus, putamen’. There was one additional pair, ‘Inferior frontal gyrus, triangular part’ and ‘Superior frontal gyrus, dorsolateral’, which appeared in all the P DFC values greater than 0.03. Pair one also appeared always when P DFC > 0.001. AAL region for pair one is already shown in the figure 19.

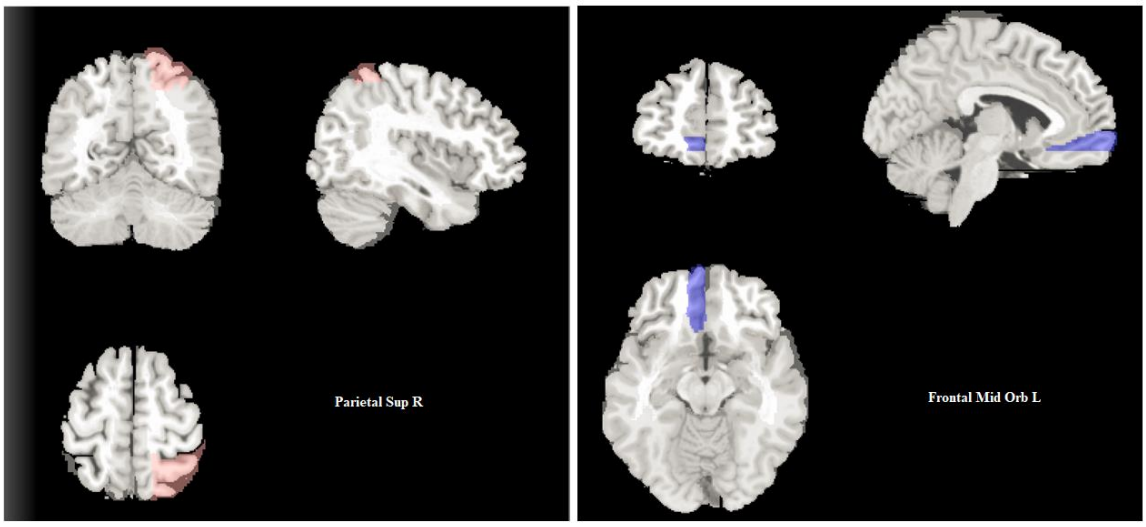

Figure 25: Pair two Parietal Sup R and Frontal Mid Orb L (AAL Region 60 and 25).

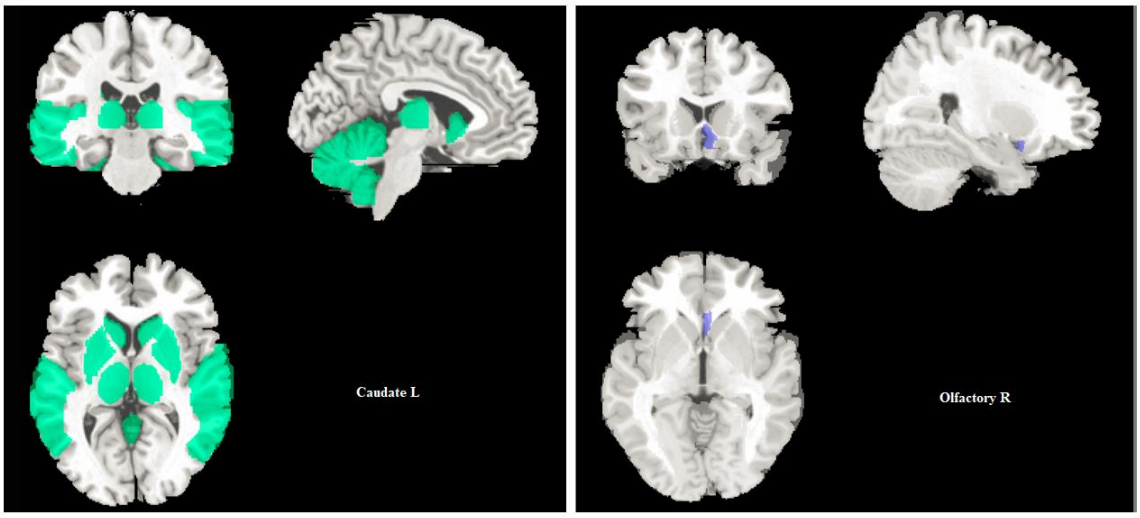

Figure 26: Pair three Left to right Caudate L and Olfactory R (AAL Region 71 and 22).

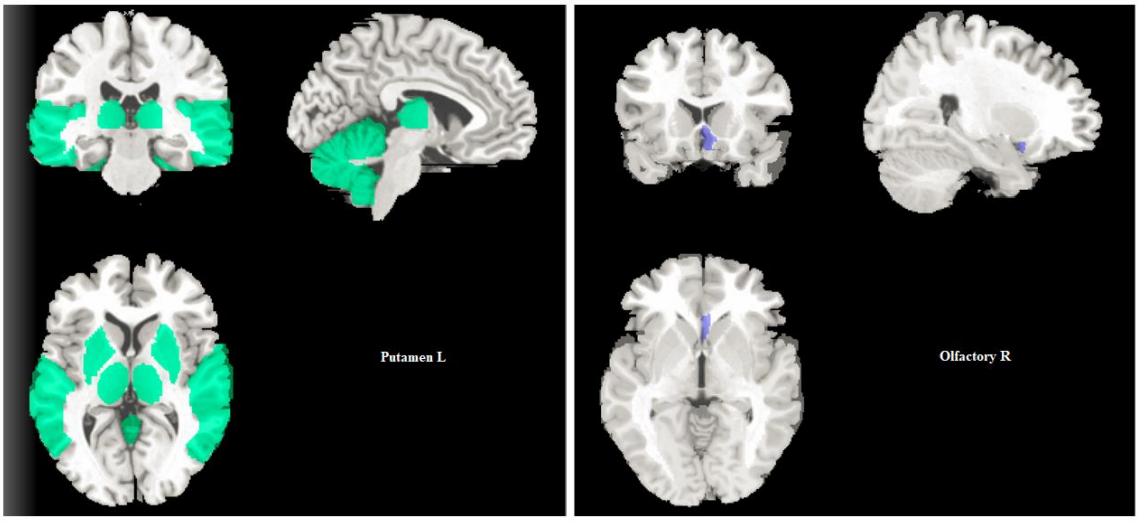

Figure 27: Pair three Left to right Putamen L and Olfactory R (AAL Region 73 and 22).

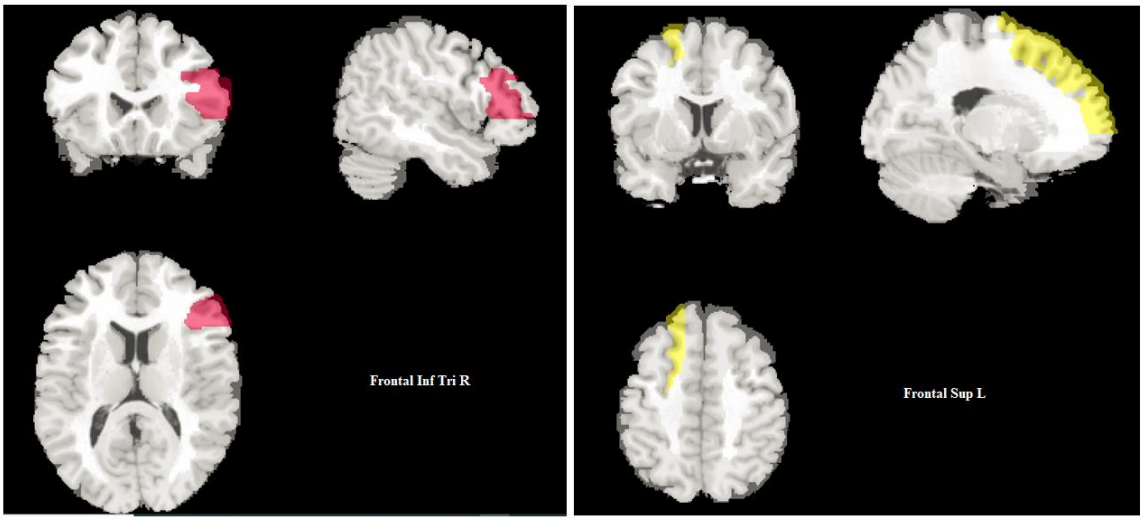

Figure 28: Pair three Left to right Frontal Inf Tri R and Frontal Sup L (AAL Region 14 and 3).

4.7. List of AAL Brain Region Pair Obtained:

This section illustrates the AAL region pair obtained for each P DFC Values. We used ten different values of P DFC, and for each P DFC value, the number of AAL region pairs obtained are listed below. Pair obtained for P DFC value 0.001 was common in all the cases.

Table 21:

Number of pairs obtained for each value of P DFC.

P DFC Value (Less Than)	Number of Pairs
0.001	2/2=1
0.002	4/2=2
0.005	8/2=4
0.01	24/2=12
0.02	64/2=32
0.03	124/2=62
0.04	174/2=87
0.05	226/2=113
0.06	298/2=149
0.1	610/2=305

Below are the lists of AAL region pairs obtained utilizing the DFC data set for maximum P DFC value of 0.05, 0.01, 0.02, 0.03, 0.001, 0.002, 0.005 and 0.04. Using appendix A, corresponding AAL region names can be obtained.

Table 22:

List of corresponding actual AAL Region Pair for max P DFC of 0.05.

PDFC	AAL Region Pair
0.05	(14 3)
	(71 3)
	(91 4)
	(25 9)
	(87 9)
	(73 10)
	(75 10)
	(101 10)
	(39 11)
	(75 11)
	(3 14)
	(95 15)
	(102 15)
	(90 19)
	(70 21)
	(73 21)
	(96 21)
	(102 21)
	(104 21)
	(106 21)
	(108 21)
	(66 22)
	(71 22)
	(73 22)
	(87 22)
	(93 22)
	(101 22)
	(106 22)
	(114 22)
	(106 23)
	(50 24)
	(82 24)
	(9 25)
	(50 25)
	(60 25)
	(35 26)
	(43 26)
	(45 26)
	(50 26)
	(75 29)
	(106 29)
	(87 30)
	(98 31)
	(100 31)
	(101 31)
	(106 31)
	(111 31)
	(42 32)
	(26 35)
	(44 36)
	(45 36)
	(46 36)
	(48 36)
	(96 36)
	(97 36)
	(11 39)
	(71 39)
	(75 39)
	(75 41)
	(95 41)
	(32 42)
	(66 42)
	(71 42)
	(26 43)
	(106 43)
	(36 44)
	(108 44)
	(26 45)
	(36 45)
	(106 45)
	(36 46)
	(108 46)
	(106 47)
	(36 48)
	(72 48)
	(104 48)
	(72 49)
	(102 49)
	(104 49)
	(24 50)
	(25 50)
	(26 50)
	(64 50)
	(106 50)
	(102 51)
	(106 51)
	(72 52)
	(102 52)
	(106 52)
	(108 52)
	(102 53)
	(106 54)
	(116 57)
	(25 60)
	(78 61)
	(102 62)
	(73 63)
	(92 63)
	(100 63)
	(104 63)
	(50 64)
	(89 64)
	(101 64)
	(116 65)
	(22 66)
	(42 66)
	(102 66)
	(21 70)

	(3 71)
	(22 71)
	(39 71)
	(42 71)
	(87 71)
	(106 71)
	(109 71)
	(48 72)
	(49 72)
	(52 72)
	(84 72)
	(10 73)
	(21 73)
	(22 73)
	(63 73)
	(110 74)
	(10 75)
	(11 75)
	(29 75)
	(39 75)
	(41 75)
	(101 77)
	(116 77)
	(61 78)
	(24 82)
	(100 83)
	(106 83)
	(72 84)
	(105 84)
	(9 87)
	(22 87)
	(30 87)
	(71 87)
	(107 87)
	(108 87)
	(116 87)
	(116 88)
	(64 89)
	(19 90)
	(101 90)

	(116 90)
	(4 91)
	(108 91)
	(63 92)
	(22 93)
	(15 95)
	(41 95)
	(115 95)
	(21 96)
	(36 96)
	(36 97)
	(31 98)
	(31 100)
	(63 100)
	(83 100)
	(10 101)
	(22 101)
	(31 101)
	(64 101)
	(77 101)
	(90 101)
	(102 101)
	(104 101)
	(15 102)
	(21 102)
	(49 102)
	(51 102)
	(52 102)
	(53 102)
	(62 102)
	(66 102)
	(101 102)
	(113 102)
	(109 103)
	(21 104)
	(48 104)
	(49 104)
	(63 104)
	(101 104)
	(84 105)

	(21 106)
	(22 106)
	(23 106)
	(29 106)
	(31 106)
	(43 106)
	(45 106)
	(47 106)
	(50 106)
	(51 106)
	(52 106)
	(54 106)
	(71 106)
	(83 106)
	(87 107)
	(21 108)
	(44 108)
	(46 108)
	(52 108)
	(87 108)
	(91 108)
	(71 109)
	(103 109)
	(110 109)
	(74 110)
	(109 110)
	(111 110)
	(31 111)
	(110 111)
	(102 113)
	(22 114)
	(95 115)
	(57 116)
	(65 116)
	(77 116)
	(87 116)
	(88 116)
	(90 116)

Table 23:

List of corresponding actual AAL Region Pair for P DFC <0.01, 0.02 and 0.03.

PDFC	AAL Region Pair
0.01	(25 9)
	(71 22)
	(73 22)
	(106 22)
	(106 23)
	(9 25)
	(50 25)
	(60 25)
	(106 31)
	(46 36)
	(75 41)
	(36 46)
	(102 49)
	(25 50)
	(102 51)
	(25 60)
	(22 71)
	(22 73)
	(41 75)
	(49 102)
	(51 102)
	(22 106)
	(23 106)
	(31 106)
PDFC 0.02	
	(25 9)
	(73 10)
	(90 19)
	(104 21)
	(106 21)
	(108 21)
	(71 22)
	(73 22)
	(87 22)
	(106 22)
	(106 23)
	(9 25)
	(50 25)
	(60 25)
	(50 26)
	(106 31)
	(46 36)
	(75 41)
	(36 46)
	(104 48)
	(102 49)
	(25 50)
	(26 50)
	(106 50)
	(102 51)
	(102 52)
	(102 53)
	(25 60)
	(102 62)
	(104 63)
	(101 64)
	(102 66)
	(22 71)
	(10 73)
	(22 73)
	(41 75)
	(116 77)
	(106 83)
	(22 87)
	(107 87)
	(116 88)
	(19 90)
	(108 91)
	(64 101)
	(49 102)
	(51 102)
	(52 102)
	(53 102)
	(62 102)
	(66 102)
	(21 104)
	(48 104)
	(63 104)
	(21 106)
	(22 106)
	(23 106)
	(31 106)
	(50 106)
	(83 106)
	(87 107)
	(21 108)
	(91 108)
	(77 116)
	(88 116)
PDFC 0.03	
	(14 3)
	(71 3)
	(25 9)
	(87 9)
	(73 10)
	(101 10)
	(39 11)
	(3 14)
	(102 15)
	(90 19)
	(73 21)
	(104 21)

	(106 21)
	(108 21)
	(66 22)
	(71 22)
	(73 22)
	(87 22)
	(101 22)
	(106 22)
	(106 23)
	(82 24)
	(9 25)
	(50 25)
	(60 25)
	(45 26)
	(50 26)
	(75 29)
	(98 31)
	(101 31)
	(106 31)
	(46 36)
	(11 39)
	(75 41)
	(66 42)
	(71 42)
	(108 44)
	(26 45)
	(106 45)
	(36 46)
	(108 46)
	(106 47)
	(104 48)
	(102 49)
	(25 50)
	(26 50)
	(106 50)
	(102 51)
	(72 52)
	(102 52)
	(106 52)
	(102 53)
	(116 57)

	(25 60)
	(102 62)
	(92 63)
	(100 63)
	(104 63)
	(101 64)
	(22 66)
	(42 66)
	(102 66)
	(3 71)
	(22 71)
	(42 71)
	(87 71)
	(106 71)
	(52 72)
	(10 73)
	(21 73)
	(22 73)
	(29 75)
	(41 75)
	(116 77)
	(24 82)
	(106 83)
	(9 87)
	(22 87)
	(71 87)
	(107 87)
	(116 88)
	(19 90)
	(116 90)
	(108 91)
	(63 92)
	(31 98)
	(63 100)
	(10 101)
	(22 101)
	(31 101)
	(64 101)
	(102 101)
	(15 102)
	(49 102)

	(51 102)
	(52 102)
	(53 102)
	(62 102)
	(66 102)
	(101 102)
	(21 104)
	(48 104)
	(63 104)
	(21 106)
	(22 106)
	(23 106)
	(31 106)
	(45 106)
	(47 106)
	(50 106)
	(52 106)
	(71 106)
	(83 106)
	(87 107)
	(21 108)
	(44 108)
	(46 108)
	(91 108)
	(110 109)
	(109 110)
	(57 116)
	(77 116)
	(88 116)
	(90 116)

Table 24:

List of corresponding actual AAL Region Pair for P DFC <0.001, 0.002 and 0.005.

P DFC	AAL Region Pair
PDFC 0.001	(50 25)
PDFC 0.002	(73 22) (50 25) (25 50) (22 73) (22 73)
PDFC 0.005	(71 22) (73 22) (50 25) (60 25) (25 50) (25 60) (22 71) (22 73)

Table 25:

Corresponding Actual AAL Region Pair for P DFC <0.04.

PDFC	AAL Region Pair
0.04	(14 3)
	(71 3)
	(91 4)
	(25 9)
	(87 9)
	(73 10)
	(75 10)
	(101 10)
	(39 11)
	(75 11)
	(3 14)
	(102 15)
	(90 19)
	(70 21)
	(73 21)
	(96 21)
	(104 21)
	(106 21)
	(108 21)
	(66 22)
	(71 22)
	(73 22)
	(87 22)
	(93 22)
	(101 22)
	(106 22)
	(114 22)
	(106 23)
	(82 24)
	(9 25)
	(50 25)
	(60 25)
	(45 26)
	(50 26)
	(75 29)
	(106 29)
	(87 30)
	(98 31)
	(100 31)
	(101 31)
	(106 31)
	(42 32)
	(44 36)
	(45 36)
	(46 36)
	(48 36)
	(11 39)
	(71 39)
	(75 39)
	(75 41)
	(32 42)
	(66 42)
	(71 42)
	(36 44)
	(108 44)
	(26 45)
	(36 45)
	(106 45)
	(36 46)
	(108 46)
	(106 47)
	(36 48)
	(104 48)
	(72 49)
	(102 49)
	(25 50)
	(26 50)
	(64 50)
	(106 50)
	(102 51)
	(106 51)
	(72 52)
	(102 52)
	(106 52)
	(102 53)
	(116 57)
	(25 60)
	(102 62)
	(92 63)
	(100 63)
	(104 63)
	(50 64)
	(89 64)
	(101 64)
	(22 66)
	(42 66)
	(102 66)
	(21 70)
	(3 71)
	(22 71)
	(39 71)
	(42 71)
	(87 71)
	(106 71)
	(49 72)
	(52 72)
	(84 72)
	(10 73)
	(21 73)
	(22 73)

	(110 74)
	(10 75)
	(11 75)
	(29 75)
	(39 75)
	(41 75)
	(116 77)
	(24 82)
	(100 83)
	(106 83)
	(72 84)
	(9 87)
	(22 87)
	(30 87)
	(71 87)
	(107 87)
	(116 88)
	(64 89)
	(19 90)
	(101 90)
	(116 90)
	(4 91)
	(108 91)
	(63 92)
	(22 93)

	(21 96)
	(31 98)
	(31 100)
	(63 100)
	(83 100)
	(10 101)
	(22 101)
	(31 101)
	(64 101)
	(90 101)
	(102 101)
	(15 102)
	(49 102)
	(51 102)
	(52 102)
	(53 102)
	(62 102)
	(66 102)
	(101 102)
	(113 102)
	(21 104)
	(48 104)
	(63 104)
	(21 106)
	(22 106)

	(23 106)
	(29 106)
	(31 106)
	(45 106)
	(47 106)
	(50 106)
	(51 106)
	(52 106)
	(71 106)
	(83 106)
	(87 107)
	(21 108)
	(44 108)
	(46 108)
	(91 108)
	(110 109)
	(74 110)
	(109 110)
	(102 113)
	(22 114)
	(57 116)
	(77 116)
	(88 116)
	(90 116)

Table 26:

Corresponding Actual AAL Region Pair for P FC <0.001 and 0.002.

P FC	**AAL Region Pair**
0.001	(116 74)
P FC 0.002	(74 36) (116 56) (116 74) (92 116) (100 116)

4.8. Discussion and Conclusion:

After analyzing the results obtained from both static FC and dynamic FC (DFC), it is evident that, dynamic functional connectivity between multiple brain networks appeared as having great group discriminating power with an average classification accuracy of up to 98%, whereas static FC-based method achieved at most 72% accuracy. The variation in the classification accuracy between DFC and FC has been presented in figure 29.

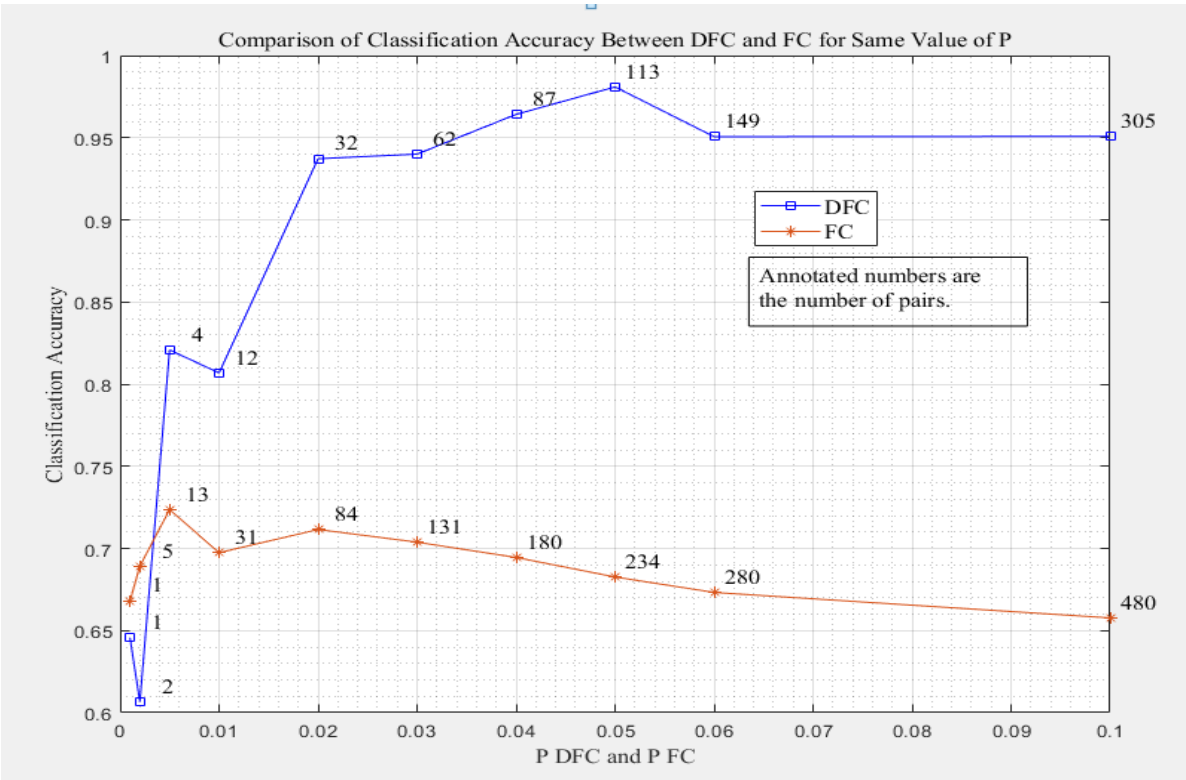

Figure 29: Comparison of classification accuracy between DFC and FC for same value of P.

It is also interesting to note that, the range of the fluctuations in the DFC between the Right Superior Occipital Gyrus and the Left Medial Orbital Superior Frontal Gyrus regions during the resting-state fMRI scan, as captured by stdDFC, was 17% lower for the GWI than the stdDFC of the NC group (significantly lower, with $p<0.001$). This

result may potentially signal an impairment for the GWI group between these regions, which are involved in functions such as visual processing, multi-sensory input processing sensorimotor processing, and semantic processing. Consistent with these findings, GWI veterans were reported to exhibit deficits word-finding, visual processing, and fine motor skills. However, brain networks involved in successful classification need to be further interpreted and studied. Ongoing and future work involves different feature selection and classification algorithms to achieve a higher classification accuracy, and more detailed study of other region-pairs involved in group discrimination. Overall, the results are in line with other recent findings of widespread impairments in resting-state FC within brain function networks implicated by multiple symptoms in GWI patients. DFC-based metrics, such as, the stdDFC in our study, with their group-discriminating differences can potentially lead to resting-state fMRI / neuroimaging biomarkers for GWI, and potentially for other neurological disorders and conditions.

CHAPTER V:

FUTURE WORK

There are different ways available to do the classification. In the future, one can directly feed the fMRI time-series data and find out the classification results or try different feature reduction methods and apply recently developed deep learning classification algorithms, such as UNet, etc.

If fMRI time-series (data stamped with timestamp) data are available, then feeding time series data directly into some prebuilt data analysis tool like SensiML [43], Google Analytics, PowerBI etc. can provide the promising results. It has good deep learning algorithms along with tools which can be customized and utilized for classification problem.

Different deep learning techniques such as AlexNet, which is similar to R-CNN can also be applied. As we could not get a good result out of R-CNN, we did not spend time trying AlexNet. If one can wisely select the parameters/options in AlexNet and reduce the features before training the network, it may give better results, however, challenging part is to select the options, parameters, and the features.

In MATLAB, one can try “The classification learner” app as well. It trains the model to classify data. Utilizing this app, one can explore supervised learning, utilizing different classifier. One challenge that can be found using a classification learner is selecting the features. In this case, close to 0.5 million features are available and training with so many features were very time-consuming. It took overnight to load all the features in the classification learner tool. If one can identify the features to be selected, then the classification learner app can be used to perform the classification.

Principal component analysis (PCA) or linear discriminant analysis (LDA) can be implemented to find out the principal components and reduce the dimension and calculate the classification.

During this research, SVM has been used, but other supervised technique can also be used. As it is explained in the results section, SVM has provided better results compared to R-CNN. It will be very interesting to see if features are obtained from the SVM t-test and feed into to R-CNN model for both DFC and FC cases.

REFERENCES

[1] "TReNDS Neuroimaging," Jul 2020. [Online]. Available: https://www.kaggle.com/c/trends-assessment-prediction.

[2] "Neuroimaging," Wikipedia, [Online]. Available: https://en.wikipedia.org/wiki/Neuroimaging.

[3] S. Huettel, A. Song and G. McCarthy, Functional Magnetic Resonance Imaging, Sinauer Associates, Sunderland, MA, 2004.

[4] "BOLD fMRI signals, time-courses," [Online].

[5] B. Biswal, J. VanKylen and J. Hyde, "Simultaneous assessment of flow and BOLD signals in resting-state functional connectivity maps," *NMR in Biomedicine,* pp. 165-170, 1997.

[6] K. Friston, "Causal Modelling and Brain Connectivity in Functional Magnetic Resonance Imaging.," *PLOS Biology,* pp. 220-225, 2009.

[7] M. Fernandez-Seara, "Effects on resting cerebral blood flow and functional connectivity induced by metoclopramide: a perfusion MRI study in healthy volunteers," *Br J Pharmacol,* 2011.

[8] S. M. Smith, "The future of FMRI connectivity," *Neuroimage,* vol. 62, no. 2, pp. 1257-1266, 2012.

[9] "Resting State fMRI," [Online]. Available: https://en.wikipedia.org/wiki/Resting_state_fMRI.

[10] K. J. Friston, "Functional and effective connectivity in neuroimaging: a synthesis," *Hum. Brain Mapp,* vol. 2, pp. 56-78, 1994.

[11] U. Sakoglu, G. D. Pearlson, K. A. Kiehl, Y. M. Wang, A. M. Michael and V. D. Calhoun, "A method for evaluating dynamic functional network connectivity and task-modulation: application to schizophrenia," *Magnetic Resonance Materials in Physics, Biology and Medicine,* vol. 23, no. 5, pp. 351-366, 2010.

[12] U. Sakoglu, B. Huisa-Garate, G. Rosenberg and R. Sood, "Application of FT-based MMSE Deconvolution Method for Cerebral Blood Flow Measurement in Patients with Leukoaraiosis," *Magnetic Resonance Imaging, Elsevier,* vol. 27, pp. 625-630, 2009.

[13] M. Pai, U. Sakoglu, S. Peterson, C. Lyons and R. Sood, "Characterization of BBB permeability in a preclinical model of cryptococcal meningoencephalitis using magnetic resonance imaging," *Journal of Cerebral Blood Flow and Metabolism,* vol. 29, pp. 545-553, 2009.

[14] U. Sakoglu, G. Pearlson, K. Kiehl and e. al, "A method for evaluating dynamic functional network connectivity and task-modulation: application to schizophrenia," *Magnetic Resonance Materials in Physics and Medicine (MAGMA),* vol. 23, no. 5, pp. 351-366, 2010.

[15] U. Sakoglu and V. Calhoun, "Temporal Dynamics of Functional Network Connectivity at Rest: A Comparison of Schizophrenia Patients and Healthy Controls," *Neuroimage,* vol. 47, 2009.

[16] S. Jampana, "Novel Time-Series Classification Analysis of EEG Data," 2015.

[17] S. Bhamidipati, "Machine Learning Applications to Classify Events from EEG Data," MS Thesis.

[18] U. Sakoglu and V. D. Calhoun, "Dynamic windowing reveals task-modulation of functional connectivity in schizophrenia patients vs healthy controls," in *ISMRM*, Honolulu, 2009.

[19] U. Sakoglu, A. Michael and C. VD, "Classification of schizophrenia patients vs healthy controls with dynamic functional network connectivity," in *Human Brain Mapping*, San Francisco, 2009.

[20] U. Sakoglu, M. Mete, J. Esquivel, K. Rubia, R. Briggs and B. Adinoff, "Classification of Cocaine Dependent Subjects with Dynamic Functional Connectivity from Functional Magnetic Resonance Imaging Data," *Journal of Neuroscience Research*, vol. 97, no. 7, pp. 790-803, 2019.

[21] R. Hutchison, T. Womelsdorf, E. Allen, P. Bandettini, V. Calhoun, M. Corbetta, P. S. Della, J. Duyn, G. Glover, J. Gonzalez-Castillo, D. Handwerker, S. Keilholz, V. Kiviniemi, D. Leopold, P. F. de, O. Sporns, M. Walter and C. Chang, "Dynamic functional connectivity: promise, issues, and interpretations," *Neuroimage*, pp. 360-378, 2013.

[22] "wikipedia," [Online]. Available: https://en.wikipedia.org/wiki/Dynamic_functional_connectivity.

[23] W. Majeed, M. Magnuson and S. D. Keilholz, "Spatiotemporal dynamics of low frequency fluctuations in BOLD fMRI of the rat," *Journal of Magnetic Resonance Imaging*, pp. 384-393, 2009.

[24] W. Majeed, M. Magnuson, W. Hasenkamp, H. Schwarb, E. H. Schumacher, L. Barsalou and S. D. Keilholz, "Spatiotemporal dynamics of low frequency BOLD fluctuations in rats and humans," *NeuroImage. ,* pp. 1140-1150, 2011.

[25] E. Tagliazucchi, P. Balenzuela, D. Fraiman, P. Montoya and D. R. Chialvo, "Spontaneous BOLD event triggered averages for estimating functional connectivity at resting state," *Neuroscience Letters,* pp. 158-163, 2011.

[26] E. Tagliazucchi, P. Balenzuela, D. Fraiman and D. R. Chialvo, "Criticality in large-scale brain fMRI dynamics unveiled by a novel point process analysis," *Frontiers in Physiology,* 2012.

[27] E. Tagliazucchi, R. Carhart-Harris, R. Leech, D. Nutt and D. R. Chialvo, "Enhanced repertoire of brain dynamical states during the psychedelic experience," *Human Brain Mapping,* 2014.

[28] E. Tagliazucchi, M. Siniatchkin, H. Laufs and D. R. Chialvo, "The voxel-wise functional connectome can be efficiently derived from co-activations in a sparse spatio-temporal point-process," *Frontiers in Neuroscience,* 2016.

[29] N. Petridou, C. C. Gaudes, I. L. Dryden, S. T. Francis and P. A. Gowland, "Periods of rest in fMRI contain individual spontaneous events which are related to slowly fluctuating spontaneous activity," *Human Brain Mapping,* vol. 34, no. 6, pp. 1319-1329, 2013.

[30] X. Liu and J. H. Duyn, "Time-varying functional network information extracted from brief instances of spontaneous brain activity".," *Proceedings of the National Academy of Sciences,* pp. 4392-4397, 2013.

[31] J. E. Chen, C. Chang, M. D. Greicius and G. H. Glover, "Introducing co-activation pattern metrics to quantify spontaneous brain network dynamics," *NeuroImage. ,* pp. 476-488, 2015.

[32] C. Chang and G. H. Glover, "Time–frequency dynamics of resting-state brain connectivity measured with fMRI," *NeuroImage. ,* pp. 81-98, 2010.

[33] "Wikipedia," [Online]. Available: https://en.wikipedia.org/wiki/Dynamic_functional_connectivity.

[34] U. Sakoglu, G. D. Pearlson, K. A. Kiehl, Y. M. Wang, A. M. Michael and V. D. Calhoun, "A method for evaluating dynamic functional network connectivity and task-modulation: application to schizophrenia," in *Magnetic Resonance Materials in Physics and Medicine (MAGMA)*, 2010.

[35] D. T. Jones, P. Vemuri, M. C. Murphy, J. L. Gunter, M. L. Senjem, M. M. Machulda, S. A. Przybelski, B. E. Gregg, K. Kantarci, D. S. Knopman, B. F. Boeve, R. C. Petersen and C. R. Jack Jr, "Non-Stationarity in the "Resting Brain's" Modular Architecture," *PLOS ONE,* 2012.

[36] K. Gopinath, U. Sakoglu, B. Crosson and R. Haley, "Exploring Brain Mechanisms Underlying Gulf War Illness with Group ICA based Analysis of fMRI Resting State Network,," *Neuroscience Letters, Elsevier*, vol. 710, pp. 136-141, 2019.

[37] "cck-law," [Online]. Available: https://cck-law.com/types-of-va-disabilities/gulf-war-syndrome/.

[38] D. Akgun, U. Sakoglu, J. Esquivel, B. Adinoff and M. Mete, "GPU accelerated dynamic functional connectivity analysis for functional MRI data," *omputerized Medical Imaging and Graphics, Elsevier,*, vol. 43, pp. 53-63, 2015.

[39] "Wikipedia," [Online]. Available: https://en.wikipedia.org/wiki/Region_Based_Convolutional_Neural_Networks.

[40] [Online]. Available: http://matlab.mathworks.com.

[41] [Online]. Available: https://www.ibm.com/docs/it/spss-modeler/SaaS?topic=models-how-svm-works.

[42] U. Sakoglu, A. Mishra, K. Gopinath, B. Crosson and R. Haley, "Classification of Gulf War Illness Patients vs Control Veterans Using fMRI Dynamic Functional Connectivity," in *ISMRM*, London, 2022.

[43] " SensiML,," SensiML, [Online]. Available: https://sensiml.com/ .

[44] N. Tzourio-Mazoyer, B. Landeau, D. Papathanassiou, F. Crivello, O. Etard, N. Delcroix and B. M. &. M. Joliot, "Automated Anatomical Labeling of activations in SPM using a Macroscopic Anatomical Parcellation of the MNI MRI single-subject brain," *NeuroImage.* , pp. 273-289, 2002.

[45] "cck-law," [Online]. Available: ttps://cck-law.com/types-of-va-disabilities/gulf-war-syndrome/.

APPENDIX A

AAL Brain Region Nomenclature [44]. The numbers after the region names represent number of voxels in the ROI.

Brain Region Label	Brain Region (ROI) Name
1	Precentral_L 2001
2	Precentral_R 2002
3	Frontal_Sup_L 2101
4	Frontal_Sup_R 2102
5	Frontal_Sup_Orb_L 2111
6	Frontal_Sup_Orb_R 2112
7	Frontal_Mid_L 2201
8	Frontal_Mid_R 2202
9	Frontal_Mid_Orb_L 2211
10	Frontal_Mid_Orb_R 2212
11	Frontal_Inf_Oper_L 2301
12	Frontal_Inf_Oper_R 2302
13	Frontal_Inf_Tri_L 2311
14	Frontal_Inf_Tri_R 2312
15	Frontal_Inf_Orb_L 2321
16	Frontal_Inf_Orb_R 2322
17	Rolandic_Oper_L 2331
18	Rolandic_Oper_R 2332
19	Supp_Motor_Area_L 2401
20	Supp_Motor_Area_R 2402
21	Olfactory_L 2501
22	Olfactory_R 2502
23	Frontal_Sup_Medial_L 2601
24	Frontal_Sup_Medial_R 2602
25	Frontal_Med_Orb_L 2611
26	Frontal_Med_Orb_R 2612
27	Rectus_L 2701
28	Rectus_R 2702

Brain Region Label	Brain Region (ROI) Name
29	Insula_L 3001
30	Insula_R 3002
31	Cingulum_Ant_L 4001
32	Cingulum_Ant_R 4002
33	Cingulum_Mid_L 4011
34	Cingulum_Mid_R 4012
35	Cingulum_Post_L 4021
36	Cingulum_Post_R 4022
37	Hippocampus_L 4101
38	Hippocampus_R 4102
39	ParaHippocampal_L 4111
40	ParaHippocampal_R 4112
41	Amygdala_L 4201
42	Amygdala_R 4202
43	Calcarine_L 5001
44	Calcarine_R 5002
45	Cuneus_L 5011
46	Cuneus_R 5012
47	Lingual_L 5021
48	Lingual_R 5022
49	Occipital_Sup_L 5101
50	Occipital_Sup_R 5102
51	Occipital_Mid_L 5201
52	Occipital_Mid_R 5202
53	Occipital_Inf_L 5301
54	Occipital_Inf_R 5302
55	Fusiform_L 5401
56	Fusiform_R 5402
57	Postcentral_L 6001
58	Postcentral_R 6002
59	Parietal_Sup_L 6101
60	Parietal_Sup_R 6102
61	Parietal_Inf_L 6201
62	Parietal_Inf_R 6202
63	SupraMarginal_L 6211

Brain Region Label	Brain Region (ROI) Name
64	SupraMarginal_R 6212
65	Angular_L 6221
66	Angular_R 6222
67	Precuneus_L 6301
68	Precuneus_R 6302
69	Paracentral_Lobule_L 6401
70	Paracentral_Lobule_R 6402
71	Caudate_L 7001
72	Caudate_R 7002
73	Putamen_L 7011
74	Putamen_R 7012
75	Pallidum_L 7021
76	Pallidum_R 7022
77	Thalamus_L 7101
78	Thalamus_R 7102
79	Heschl_L 8101
80	Heschl_R 8102
81	Temporal_Sup_L 8111
82	Temporal_Sup_R 8112
83	Temporal_Pole_Sup_L 8121
84	Temporal_Pole_Sup_R 8122
85	Temporal_Mid_L 8201
86	Temporal_Mid_R 8202
87	Temporal_Pole_Mid_L 8211
88	Temporal_Pole_Mid_R 8212
89	Temporal_Inf_L 8301
90	Temporal_Inf_R 8302
91	Cerebelum_Crus1_L 9001
92	Cerebelum_Crus1_R 9002
93	Cerebelum_Crus2_L 9011
94	Cerebelum_Crus2_R 9012

Brain Region Label	Brain Region (ROI) Name
95	Cerebelum_3_L 9021
96	Cerebelum_3_R 9022
97	Cerebelum_4_5_L 9031
98	Cerebelum_4_5_R 9032
99	Cerebelum_6_L 9041
100	Cerebelum_6_R 9042
101	Cerebelum_7b_L 9051
102	Cerebelum_7b_R 9052
103	Cerebelum_8_L 9061
104	Cerebelum_8_R 9062
105	Cerebelum_9_L 9071
106	Cerebelum_9_R 9072
107	Cerebelum_10_L 9081
108	Cerebelum_10_R 9082
109	Vermis_1_2 9100
110	Vermis_3 9110
111	Vermis_4_5 9120
112	Vermis_6 9130
113	Vermis_7 9140
114	Vermis_8 9150
115	Vermis_9 9160
116	Vermis_10 9170

APPENDIX B

This section contains the list of all indices of a brain region pair obtained for P DFC Values. Each index represent a brain region pair (I and J). One can obtained I and J values using below formula in MATLAB.

[I J] = ind2sub (116, indices).

Here the value I and J represent the AAL brain region.

P-DFC Values and Corresponding AAL Region Indices										
P-DFC →	0.001	0.002	0.005	0.01	0.02	0.03	0.04	0.05	0.06	0.1
Indices↓	2834	2509	2507	953	953	246	246	246	102	55
	5709	2834	2509	2507	1117	303	303	303	246	100
		5709	2834	2509	2178	953	439	439	303	101
		8374	2844	2542	2424	1015	953	953	439	102
			5709	2658	2426	1117	1015	1015	440	116
			6869	2793	2428	1145	1117	1117	452	182
			8142	2834	2507	1199	1119	1119	602	232
			8374	2844	2509	1511	1145	1145	686	246
				3586	2523	1726	1199	1199	696	303
				4106	2542	2178	1235	1235	797	348
				4715	2658	2393	1511	1511	903	358
				5256	2793	2424	1726	1719	953	439
				5670	2834	2426	2178	1726	1015	440
				5709	2844	2428	2390	2178	1056	448
				5902	2950	2502	2393	2390	1117	452
				6869	3586	2507	2416	2393	1119	480
				8142	4106	2509	2424	2416	1145	602
				8374	4715	2523	2426	2422	1199	686
				8625	5256	2537	2428	2424	1235	696
				11765	5556	2542	2502	2426	1286	738
				11767	5670	2658	2507	2428	1511	797
				12202	5709	2750	2509	2502	1719	903
				12203	5710	2793	2523	2507	1726	916
				12211	5790	2834	2529	2509	2175	953

P-DFC Values and Corresponding AAL Region Indices							
		5902	2844	2537	2523	2178	954
		6018	2945	2542	2529	2390	1000
		6134	2950	2550	2537	2393	1006
		6869	3323	2658	2542	2416	1015
		7178	3578	2750	2550	2421	1048
		7296	3581	2793	2658	2422	1056
		7409	3586	2834	2718	2424	1066
		7642	4106	2844	2750	2426	1105
		8142	4419	2945	2793	2428	1117
		8362	4715	2950	2834	2442	1119
		8374	4822	3323	2844	2502	1145
		8625	4827	3354	2935	2507	1179
		8932	5096	3451	2943	2509	1185
		9618	5130	3578	2945	2514	1199
		9998	5210	3580	2950	2519	1235
		10083	5256	3581	3323	2523	1261
		10208	5328	3586	3354	2529	1286
		10343	5442	3638	3451	2537	1470
		10548	5556	4104	3578	2542	1493
		11664	5670	4105	3580	2550	1498
		11765	5709	4106	3581	2658	1511
		11767	5710	4108	3586	2718	1581
		11768	5790	4419	3591	2750	1701
		11769	5902	4479	3638	2793	1719
		11778	5988	4483	3970	2833	1724
		11782	6018	4715	4104	2834	1726
		11969	6022	4788	4105	2844	1736
		11996	6134	4822	4106	2935	1745
		12011	6612	4827	4108	2943	1776
		12201	6869	5024	4156	2945	1848
		12202	7178	5096	4157	2949	1878
		12203	7284	5130	4419	2950	1881
		12211	7292	5140	4479	3239	1895
		12230	7296	5210	4483	3323	1921
		12263	7409	5256	4715	3354	1943
		12383	7562	5328	4735	3451	1956
		12433	7582	5442	4788	3578	1972

P-DFC Values and Corresponding AAL Region Indices							
		12503	7642	5488	4822	3580	2099
		13417	8123	5556	4827	3581	2175
		13428	8142	5640	4898	3582	2178
			8162	5670	4978	3584	2204
			8207	5709	5024	3586	2291
			8226	5710	5096	3591	2320
			8288	5748	5130	3638	2390
			8362	5790	5140	3897	2392
			8373	5902	5210	3915	2393
			8374	5906	5256	3970	2414
			8613	5988	5328	4104	2416
			8625	6018	5442	4105	2421
			8932	6022	5488	4106	2422
			9420	6134	5524	4108	2424
			9618	6612	5556	4156	2426
			9985	6869	5640	4157	2428
			9998	7178	5670	4276	2442
			10047	7284	5672	4419	2446
			10083	7292	5708	4479	2453
			10208	7296	5709	4483	2474
			10343	7358	5710	4715	2475
			10440	7397	5748	4735	2489
			10548	7409	5790	4788	2495
			10619	7562	5902	4822	2496
			11283	7582	5906	4827	2501
			11547	7642	5988	4898	2502
			11610	8025	6018	4976	2507
			11622	8123	6022	4978	2509
			11631	8142	6024	5024	2514
			11664	8159	6134	5096	2519
			11702	8162	6254	5130	2523
			11731	8207	6612	5140	2528
			11765	8226	6869	5210	2529
			11767	8285	7038	5256	2530
			11768	8288	7178	5328	2531
			11769	8320	7265	5442	2537
			11778	8362	7284	5488	2542

P-DFC Values and Corresponding AAL Region Indices						
		11782	8373	7292	5524	2543
		11817	8374	7296	5556	2550
		11969	8578	7358	5593	2640
		11996	8594	7397	5594	2644
		12011	8595	7409	5640	2658
		12201	8613	7540	5670	2698
		12202	8623	7562	5672	2717
		12203	8625	7582	5708	2718
		12211	8932	7642	5709	2750
		12225	9420	8025	5710	2754
		12227	9612	8123	5748	2774
		12230	9618	8142	5790	2793
		12232	9700	8159	5797	2795
		12251	9985	8162	5902	2801
		12263	9998	8207	5906	2815
		12383	10006	8226	5988	2822
		12433	10047	8229	6018	2833
		12456	10083	8284	6020	2834
		12458	10208	8285	6022	2837
		12503	10272	8288	6024	2844
		12638	10343	8320	6134	2845
		12753	10425	8362	6231	2856
		13397	10440	8373	6250	2909
		13417	10444	8374	6254	2935
		13428	10548	8415	6612	2943
		13430	10619	8578	6869	2945
			10694	8594	6931	2946
			11041	8595	6939	2949
			11283	8613	7038	2950
			11515	8623	7061	2953
			11547	8625	7178	2979
			11567	8917	7265	3009
			11610	8932	7284	3013
			11622	8993	7292	3180
			11631	9420	7296	3239
			11664	9612	7358	3323
			11690	9618	7397	3335

P-DFC Values and Corresponding AAL Region Indices					
		11702	9700	7409	3354
		11731	9733	7540	3388
		11765	9985	7562	3400
		11767	9998	7582	3451
		11768	10006	7641	3505
		11769	10047	7642	3522
		11778	10083	7762	3547
		11782	10084	7922	3558
		11817	10092	8025	3578
		11829	10208	8123	3580
		11969	10272	8142	3581
		11996	10343	8159	3582
		12011	10425	8162	3584
		12201	10440	8207	3586
		12202	10444	8226	3591
		12203	10548	8229	3638
		12209	10619	8284	3697
		12211	10694	8285	3781
		12225	10919	8288	3897
		12227	10945	8320	3915
		12230	11019	8337	3970
		12231	11041	8362	3989
		12232	11056	8373	3993
		12251	11172	8374	4028
		12263	11283	8415	4032
		12383	11515	8573	4049
		12433	11547	8578	4076
		12456	11567	8594	4090
		12458	11610	8595	4102
		12503	11622	8613	4104
		12638	11631	8623	4105
		12718	11664	8625	4106
		12753	11677	8700	4107
		13094	11690	8907	4108
		13130	11702	8917	4109
		13397	11704	8932	4110
		13417	11731	8954	4124

P-DFC Values and Corresponding AAL Region Indices					
		13428	11737	8993	4128
		13430	11765	9420	4156
			11767	9534	4157
			11768	9566	4171
			11769	9612	4248
			11778	9618	4276
			11782	9700	4278
			11817	9733	4282
			11829	9985	4288
			11941	9995	4314
			11969	9998	4317
			11996	10006	4419
			11997	10010	4425
			12011	10036	4430
			12049	10047	4479
			12148	10083	4483
			12201	10084	4513
			12202	10092	4595
			12203	10208	4715
			12209	10272	4735
			12211	10343	4763
			12223	10425	4787
			12225	10440	4788
			12227	10444	4792
			12230	10448	4822
			12231	10517	4827
			12232	10544	4836
			12234	10548	4852
			12251	10560	4898
			12263	10619	4976
			12383	10694	4978
			12433	10919	5024
			12456	10945	5092
			12458	10964	5096
			12464	11019	5130
			12499	11041	5139
			12503	11056	5140

P-DFC Values and Corresponding AAL Region Indices				
		12599	11172	5169
		12631	11283	5210
		12638	11515	5246
		12718	11521	5256
		12753	11547	5287
		12755	11567	5307
		12791	11607	5324
		12870	11610	5328
		13094	11621	5372
		13130	11622	5408
		13319	11631	5442
		13397	11661	5480
		13405	11664	5488
		13417	11666	5524
		13427	11672	5556
		13428	11677	5592
		13430	11690	5593
			11702	5594
			11704	5603
			11717	5604
			11731	5640
			11737	5670
			11747	5672
			11765	5674
			11767	5708
			11768	5709
			11769	5710
			11770	5720
			11778	5748
			11782	5786
			11817	5790
			11829	5797
			11941	5872
			11952	5902
			11969	5904
			11979	5906
			11991	5979

P-DFC Values and Corresponding AAL Region Indices			
		11996	5988
		11997	6012
		12000	6014
		12011	6018
		12039	6020
		12049	6022
		12138	6024
		12148	6054
		12186	6057
		12201	6058
		12202	6130
		12203	6134
		12209	6136
		12211	6138
		12223	6231
		12225	6250
		12227	6254
		12230	6265
		12231	6366
		12232	6380
		12234	6597
		12247	6612
		12251	6728
		12263	6750
		12324	6800
		12383	6811
		12433	6866
		12456	6869
		12458	6911
		12464	6931
		12499	6939
		12503	6970
		12599	6985
		12631	7038
		12638	7061
		12718	7143
		12753	7178

P-DFC Values and Corresponding AAL Region Indices			
		12755	7244
		12791	7257
		12870	7265
		13042	7284
		13094	7292
		13130	7293
		13319	7296
		13346	7300
		13397	7344
		13405	7358
		13415	7374
		13417	7397
		13427	7409
		13428	7441
		13430	7446
			7469
			7487
			7540
			7542
			7562
			7582
			7604
			7641
			7642
			7687
			7702
			7716
			7718
			7762
			7808
			7921
			7922
			7958
			8004
			8025
			8073
			8123

P-DFC Values and Corresponding AAL Region Indices		
		8142
		8159
		8160
		8162
		8207
		8226
		8229
		8245
		8257
		8261
		8273
		8283
		8284
		8285
		8287
		8288
		8295
		8320
		8337
		8362
		8366
		8373
		8374
		8415
		8430
		8573
		8578
		8594
		8595
		8613
		8623
		8625
		8671
		8700
		8788
		8808
		8831

P-DFC Values and Corresponding AAL Region Indices		
		8907
		8917
		8918
		8920
		8932
		8941
		8945
		8954
		8963
		8993
		9005
		9015
		9019
		9074
		9206
		9380
		9420
		9497
		9534
		9566
		9571
		9590
		9612
		9618
		9663
		9700
		9733
		9836
		9844
		9846
		9848
		9884
		9958
		9961
		9976
		9985
		9993

P-DFC Values and Corresponding AAL Region Indices		
		9995
		9996
		9998
		10005
		10006
		10010
		10022
		10036
		10047
		10051
		10054
		10083
		10084
		10085
		10092
		10115
		10127
		10168
		10208
		10272
		10323
		10343
		10425
		10432
		10440
		10444
		10448
		10517
		10542
		10544
		10548
		10560
		10578
		10579
		10619
		10641
		10657

P-DFC Values and Corresponding AAL Region Indices		
		10694
		10809
		10810
		10919
		10926
		10945
		10964
		11002
		11009
		11019
		11041
		11056
		11062
		11072
		11172
		11283
		11304
		11305
		11338
		11347
		11476
		11485
		11488
		11499
		11501
		11515
		11521
		11547
		11565
		11567
		11569
		11585
		11601
		11607
		11610
		11611
		11613

P-DFC Values and Corresponding AAL Region Indices		
		11621
		11622
		11631
		11632
		11657
		11661
		11663
		11664
		11666
		11672
		11677
		11682
		11686
		11690
		11692
		11700
		11702
		11704
		11717
		11731
		11737
		11747
		11753
		11765
		11766
		11767
		11768
		11769
		11770
		11771
		11778
		11782
		11793
		11801
		11807
		11817
		11829

P-DFC Values and Corresponding AAL Region Indices		
		11941
		11948
		11952
		11956
		11969
		11979
		11991
		11992
		11994
		11996
		11997
		11999
		12000
		12001
		12011
		12025
		12033
		12039
		12049
		12099
		12103
		12138
		12148
		12159
		12173
		12186
		12193
		12201
		12202
		12203
		12204
		12209
		12211
		12217
		12223
		12225
		12227

P-DFC Values and Corresponding AAL Region Indices		
		12229
		12230
		12231
		12232
		12233
		12234
		12247
		12251
		12263
		12318
		12324
		12383
		12428
		12433
		12456
		12458
		12464
		12475
		12488
		12499
		12502
		12503
		12511
		12554
		12599
		12615
		12631
		12633
		12638
		12639
		12718
		12753
		12755
		12791
		12796
		12869
		12870

P-DFC Values and Corresponding AAL Region Indices		
		12875
		12891
		12913
		13018
		13042
		13094
		13108
		13130
		13313
		13319
		13335
		13341
		13342
		13343
		13346
		13357
		13359
		13360
		13395
		13397
		13398
		13405
		13409
		13415
		13417
		13426
		13427
		13428
		13430
		13443
		13453

APPENDIX C

This section contains the list of all indices of a brain region pair obtained for certain P FC Values. Each index represent a brain region pair (I and J). Below formula can be utilized to obtained I and J values in MATLAB.

[I J] = ind2sub (116, indices). Here the value I and J represent the AAL brain region.

P-FC Values and Corresponding AAL Region Indices										
P-FC →	**0.001**	**0.002**	**0.005**	**0.01**	**0.02**	**0.03**	**0.04**	**0.05**	**0.06**	**0.1**
	8584	4134	3480	1392	205	15	15	15	15	9
	13414	6496	4134	3480	232	205	205	151	151	15
		8504	4408	4003	552	232	232	182	182	151
		8584	5044	4018	928	552	348	205	205	152
		10672	6032	4134	1392	928	480	225	213	182
		11600	6264	4136	1677	1365	506	232	225	191
		13396	6424	4395	1681	1391	552	348	232	194
		13414	6496	4408	3248	1392	572	480	348	205
		13432	8504	4633	3321	1624	928	506	480	213
Indices↓		13440	8584	4640	3399	1625	1160	540	506	219
			10672	5044	3400	1677	1365	551	540	221
			11484	5800	3479	1681	1391	552	551	225
			11600	6032	3480	1856	1392	572	552	232
			11948	6264	3781	3241	1623	812	568	320
			12528	6424	3782	3248	1624	928	572	341
			13370	6496	3898	3321	1625	1133	812	348
			13378	6763	3917	3399	1641	1160	928	464
			13392	8352	3974	3400	1667	1365	1032	474
			13394	8503	4000	3438	1675	1391	1133	476
			13396	8504	4003	3479	1677	1392	1160	480
			13414	8577	4004	3480	1681	1466	1365	501
			13432	8578	4008	3747	1703	1623	1391	504
			13439	8583	4014	3781	1709	1624	1392	505
			13440	8584	4018	3782	1745	1625	1466	506
			13443	8736	4090	3863	1849	1641	1623	540

P-FC Values and Corresponding AAL Region Indices									
		13448	8810	4098	3898	1856	1667	1624	548
			8816	4116	3917	1871	1671	1625	551
			9976	4134	3974	2088	1675	1641	552
			10433	4136	3977	2111	1677	1667	560
			10672	4328	3978	2163	1681	1671	562
			10904	4368	4000	2571	1703	1675	568
			11252	4375	4003	3241	1709	1677	571
			11484	4390	4004	3248	1745	1681	572
			11600	4395	4008	3321	1849	1703	621
			11870	4401	4012	3322	1856	1705	655
			11948	4408	4013	3399	1871	1709	696
			12528	4524	4014	3400	2088	1745	805
			12568	4633	4018	3430	2111	1849	811
			12602	4639	4090	3438	2163	1856	812
			12618	4640	4098	3473	2571	1871	841
			12718	4865	4116	3479	2810	2088	927
			12720	4872	4134	3480	2925	2111	928
			13298	4919	4136	3747	3241	2163	929
			13352	5044	4328	3781	3248	2571	985
			13370	5379	4368	3782	3321	2810	1006
			13378	5568	4375	3863	3322	2925	1030
			13380	5800	4390	3898	3323	3241	1032
			13390	6032	4392	3917	3399	3247	1036
			13392	6047	4395	3974	3400	3248	1049
			13394	6264	4397	3977	3408	3321	1133
			13396	6415	4401	3978	3430	3322	1160
			13412	6416	4407	3983	3438	3323	1233
			13414	6424	4408	4000	3439	3364	1281
			13416	6495	4517	4002	3473	3399	1311
			13426	6496	4524	4003	3479	3400	1365
			13432	6511	4633	4004	3480	3408	1381
			13434	6763	4634	4008	3747	3430	1391
			13437	6879	4639	4012	3781	3438	1392
			13439	7343	4640	4013	3782	3439	1410
			13440	7397	4749	4014	3801	3473	1449
			13443	7888	4865	4018	3863	3479	1466
			13448	7921	4871	4090	3898	3480	1467

P-FC Values and Corresponding AAL Region Indices							
		8037	4872	4098	3917	3747	1617
		8038	4919	4100	3946	3781	1623
		8039	5036	4116	3974	3782	1624
		8352	5044	4124	3977	3801	1625
		8381	5104	4134	3978	3863	1641
		8468	5336	4136	3983	3897	1667
		8503	5379	4328	3994	3898	1668
		8504	5452	4368	4000	3917	1671
		8557	5496	4375	4002	3946	1672
		8577	5568	4390	4003	3974	1675
		8578	5800	4391	4004	3977	1677
		8579	6032	4392	4008	3978	1681
		8583	6047	4395	4011	3983	1689
		8584	6264	4397	4012	3994	1703
		8666	6415	4401	4013	4000	1705
		8736	6416	4402	4014	4002	1709
		8738	6424	4403	4018	4003	1745
		8805	6489	4407	4034	4004	1775
		8809	6495	4408	4090	4006	1797
		8810	6496	4443	4098	4008	1849
		8816	6511	4483	4100	4011	1855
		9471	6763	4517	4116	4012	1856
		9512	6879	4518	4124	4013	1871
		9550	7192	4524	4134	4014	1929
		9976	7343	4560	4136	4018	1985
		10097	7397	4633	4328	4034	2038
		10201	7424	4634	4348	4090	2061
		10210	7807	4639	4368	4098	2071
		10242	7888	4640	4370	4100	2073
		10272	7921	4749	4375	4116	2077
		10282	7923	4761	4390	4124	2088
		10433	7958	4865	4391	4134	2111
		10440	8037	4871	4392	4136	2163
		10672	8038	4872	4395	4158	2195
		10904	8039	4887	4397	4328	2235
		11252	8073	4919	4401	4348	2262
		11290	8093	4926	4402	4366	2279

P-FC Values and Corresponding AAL Region Indices							
		11358	8113	5036	4403	4368	2288
		11362	8236	5044	4407	4370	2293
		11484	8352	5104	4408	4375	2320
		11599	8381	5336	4443	4388	2571
		11600	8441	5379	4483	4390	2576
		11870	8457	5452	4517	4391	2691
		11948	8468	5496	4518	4392	2697
		12064	8498	5568	4524	4395	2784
		12140	8503	5621	4560	4397	2810
		12278	8504	5800	4633	4401	2925
		12405	8551	5815	4634	4402	3009
		12412	8557	5901	4639	4403	3016
		12527	8567	6032	4640	4407	3227
		12528	8571	6047	4749	4408	3237
		12566	8573	6081	4761	4443	3241
		12568	8577	6148	4865	4483	3243
		12570	8578	6191	4871	4517	3247
		12602	8579	6241	4872	4518	3248
		12604	8580	6264	4887	4524	3256
		12616	8583	6415	4919	4560	3272
		12618	8584	6416	4926	4627	3321
		12635	8666	6424	5018	4633	3322
		12718	8736	6489	5036	4634	3323
		12720	8738	6495	5044	4635	3361
		12742	8803	6496	5104	4639	3363
		12834	8805	6511	5336	4640	3364
		12990	8809	6647	5351	4749	3399
		12991	8810	6763	5379	4761	3400
		12992	8816	6879	5452	4865	3408
		13220	9471	7192	5496	4871	3430
		13254	9512	7343	5508	4872	3437
		13264	9550	7344	5568	4887	3438
		13280	9586	7397	5621	4919	3439
		13298	9744	7424	5669	4926	3440
		13324	9976	7570	5719	5018	3453
		13332	10097	7807	5793	5036	3473
		13336	10201	7888	5800	5044	3474

P-FC Values and Corresponding AAL Region Indices							
		13342	10208	7921	5815	5104	3475
		13348	10210	7923	5901	5336	3476
		13352	10220	7958	5916	5351	3479
		13368	10242	7997	6032	5379	3480
		13370	10272	8037	6047	5452	3500
		13378	10278	8038	6081	5496	3569
		13379	10281	8039	6148	5508	3747
		13380	10282	8073	6191	5568	3781
		13382	10433	8093	6241	5621	3782
		13388	10440	8113	6264	5669	3801
		13390	10556	8236	6415	5719	3863
		13392	10671	8346	6416	5793	3897
		13394	10672	8351	6418	5800	3898
		13396	10788	8352	6424	5815	3917
		13408	10904	8381	6428	5901	3925
		13412	11118	8441	6448	5916	3937
		13413	11252	8457	6456	6032	3946
		13414	11290	8467	6489	6047	3956
		13416	11348	8468	6492	6081	3960
		13422	11358	8497	6495	6133	3974
		13426	11362	8498	6496	6148	3977
		13430	11368	8503	6511	6191	3978
		13432	11442	8504	6647	6241	3983
		13434	11483	8551	6728	6264	3984
		13437	11484	8557	6763	6415	3990
		13439	11522	8567	6795	6416	3994
		13440	11599	8571	6879	6418	4000
		13443	11600	8573	7175	6424	4002
		13444	11716	8577	7192	6428	4003
		13447	11870	8578	7343	6442	4004
		13448	11906	8579	7344	6446	4006
		13452	11908	8580	7374	6448	4008
			11948	8583	7397	6456	4011
			12064	8584	7413	6479	4012
			12102	8603	7424	6480	4013
			12137	8623	7542	6489	4014
			12138	8666	7570	6491	4018

P-FC Values and Corresponding AAL Region Indices						
		12140	8736	7604	6492	4020
		12180	8738	7691	6495	4026
		12278	8782	7715	6496	4028
		12405	8803	7731	6511	4034
		12412	8805	7807	6647	4042
		12527	8809	7828	6728	4047
		12528	8810	7881	6763	4049
		12556	8811	7888	6795	4062
		12566	8815	7921	6879	4090
		12567	8816	7923	7111	4098
		12568	9048	7958	7132	4100
		12569	9063	7983	7175	4102
		12570	9471	7985	7185	4116
		12584	9472	7997	7192	4124
		12598	9512	8037	7343	4128
		12602	9550	8038	7344	4134
		12604	9586	8039	7374	4136
		12616	9599	8073	7397	4158
		12618	9744	8093	7405	4181
		12635	9759	8113	7407	4251
		12684	9976	8236	7413	4328
		12718	10059	8325	7423	4348
		12720	10097	8345	7424	4366
		12742	10201	8346	7542	4367
		12834	10208	8347	7570	4368
		12950	10210	8351	7596	4370
		12990	10220	8352	7604	4375
		12991	10242	8381	7622	4388
		12992	10272	8441	7691	4389
		13220	10278	8457	7715	4390
		13236	10281	8467	7731	4391
		13254	10282	8468	7765	4392
		13262	10433	8481	7807	4393
		13264	10440	8497	7828	4395
		13266	10556	8498	7881	4397
		13280	10671	8503	7888	4401

P-FC Values and Corresponding AAL Region Indices						
		13298	10672	8504	7921	4402
		13316	10726	8551	7922	4403
		13323	10788	8557	7923	4407
		13324	10894	8565	7958	4408
		13332	10904	8567	7977	4443
		13336	11118	8571	7983	4483
		13342	11131	8573	7985	4491
		13348	11252	8577	7997	4517
		13352	11290	8578	8037	4518
		13354	11348	8579	8038	4523
		13356	11358	8580	8039	4524
		13368	11362	8583	8073	4529
		13370	11368	8584	8093	4559
		13378	11406	8603	8113	4560
		13379	11442	8613	8229	4607
		13380	11483	8614	8236	4624
		13382	11484	8623	8325	4627
		13384	11522	8651	8345	4629
		13386	11599	8666	8346	4633
		13387	11600	8670	8347	4634
		13388	11651	8674	8351	4635
		13390	11716	8689	8352	4639
		13392	11870	8705	8381	4640
		13394	11906	8736	8427	4645
		13396	11908	8738	8441	4646
		13402	11941	8756	8457	4715
		13404	11947	8782	8467	4749
		13408	11948	8792	8468	4761
		13411	12054	8799	8481	4792
		13412	12064	8803	8497	4865
		13413	12102	8805	8498	4871
		13414	12137	8809	8503	4872
		13416	12138	8810	8504	4887
		13422	12140	8811	8506	4919
		13424	12180	8815	8551	4926
		13426	12274	8816	8557	4928
		13428	12278	8932	8565	4988

P-FC Values and Corresponding AAL Region Indices						
		13430	12284	8970	8567	5003
		13431	12288	9021	8571	5018
		13432	12405	9048	8573	5036
		13433	12412	9063	8577	5042
		13434	12417	9471	8578	5044
		13437	12518	9472	8579	5104
		13438	12527	9512	8580	5169
		13439	12528	9550	8582	5179
		13440	12544	9586	8583	5213
		13441	12556	9599	8584	5220
		13443	12558	9737	8603	5255
		13444	12566	9744	8613	5276
		13445	12567	9759	8614	5294
		13447	12568	9935	8623	5296
		13448	12569	9969	8651	5329
		13452	12570	9976	8657	5336
			12584	9981	8666	5351
			12597	10059	8667	5379
			12598	10085	8670	5390
			12602	10097	8674	5452
			12604	10201	8689	5467
			12616	10208	8700	5496
			12618	10210	8705	5508
			12631	10218	8736	5568
			12635	10220	8738	5619
			12682	10241	8756	5621
			12683	10242	8782	5669
			12684	10272	8783	5719
			12716	10278	8788	5749
			12718	10280	8792	5793
			12720	10281	8798	5800
			12742	10282	8799	5815
			12798	10286	8803	5849
			12834	10359	8805	5893
			12836	10399	8809	5901
			12856	10433	8810	5912
			12950	10440	8811	5916

P-FC Values and Corresponding AAL Region Indices					
		12990	10556	8815	6025
		12991	10632	8816	6032
		12992	10671	8932	6047
		13220	10672	8970	6081
		13224	10726	9021	6125
		13236	10788	9048	6133
		13238	10894	9063	6144
		13254	10904	9295	6147
		13262	10973	9462	6148
		13264	11118	9471	6191
		13266	11131	9472	6192
		13280	11205	9495	6195
		13296	11210	9505	6239
		13297	11252	9511	6241
		13298	11290	9512	6249
		13300	11348	9550	6263
		13316	11358	9586	6264
		13323	11362	9587	6380
		13324	11368	9588	6415
		13327	11406	9599	6416
		13332	11430	9737	6418
		13336	11442	9744	6423
		13340	11444	9759	6424
		13342	11483	9935	6426
		13343	11484	9969	6428
		13348	11522	9975	6442
		13350	11590	9976	6444
		13352	11599	9981	6446
		13354	11600	10059	6448
		13356	11649	10085	6453
		13358	11651	10097	6454
		13368	11716	10168	6456
		13370	11870	10201	6479
		13378	11906	10208	6480
		13379	11908	10210	6486
		13380	11937	10218	6489
		13382	11941	10220	6490

P-FC Values and Corresponding AAL Region Indices					
		13384	11947	10241	6491
		13386	11948	10242	6492
		13387	12054	10272	6495
		13388	12064	10277	6496
		13390	12102	10278	6505
		13392	12128	10280	6509
		13393	12137	10281	6511
		13394	12138	10282	6512
		13396	12139	10286	6580
		13402	12140	10359	6632
		13404	12167	10399	6647
		13408	12180	10433	6701
		13411	12274	10439	6721
		13412	12278	10440	6728
		13413	12280	10556	6763
		13414	12284	10632	6795
		13416	12288	10665	6837
		13418	12405	10671	6879
		13422	12406	10672	6928
		13424	12412	10726	6953
		13426	12417	10788	7111
		13428	12518	10894	7132
		13430	12522	10903	7159
		13431	12527	10904	7165
		13432	12528	10973	7175
		13433	12530	11058	7181
		13434	12544	11118	7185
		13437	12556	11130	7192
		13438	12558	11131	7343
		13439	12566	11138	7344
		13440	12567	11200	7364
		13441	12568	11205	7374
		13443	12569	11210	7378
		13444	12570	11245	7383
		13445	12578	11252	7397
		13447	12584	11288	7402
		13448	12596	11290	7405

P-FC Values and Corresponding AAL Region Indices					
		13452	12597	11328	7407
		13454	12598	11348	7411
		13455	12600	11358	7413
			12602	11361	7417
			12604	11362	7423
			12612	11368	7424
			12614	11406	7439
			12615	11424	7469
			12616	11430	7474
			12618	11432	7497
			12631	11442	7536
			12635	11444	7540
			12682	11450	7542
			12683	11483	7558
			12684	11484	7570
			12716	11522	7596
			12718	11540	7604
			12720	11590	7614
			12742	11594	7616
			12751	11599	7622
			12752	11600	7626
			12798	11649	7630
			12832	11651	7656
			12834	11653	7691
			12836	11716	7715
			12856	11870	7730
			12876	11872	7731
			12932	11906	7765
			12950	11908	7807
			12990	11937	7808
			12991	11941	7828
			12992	11947	7846
			13220	11948	7848
			13224	11953	7871
			13236	11957	7877
			13238	12054	7881
			13254	12064	7888

P-FC Values and Corresponding AAL Region Indices				
		13262	12102	7921
		13264	12128	7922
		13266	12137	7923
		13280	12138	7958
		13296	12139	7963
		13297	12140	7977
		13298	12167	7983
		13300	12180	7985
		13316	12274	7997
		13323	12278	8037
		13324	12280	8038
		13327	12284	8039
		13332	12288	8068
		13336	12405	8073
		13340	12406	8093
		13342	12412	8101
		13343	12417	8113
		13347	12518	8120
		13348	12522	8229
		13350	12527	8235
		13352	12528	8236
		13354	12530	8325
		13356	12544	8332
		13358	12556	8345
		13368	12558	8346
		13370	12566	8347
		13378	12567	8351
		13379	12568	8352
		13380	12569	8363
		13382	12570	8369
		13384	12578	8381
		13386	12584	8382
		13387	12590	8408
		13388	12595	8417
		13390	12596	8427
		13391	12597	8433
		13392	12598	8441

P-FC Values and Corresponding AAL Region Indices				
		13393	12599	8451
		13394	12600	8453
		13396	12602	8455
		13398	12604	8457
		13402	12610	8467
		13404	12612	8468
		13408	12614	8481
		13411	12615	8497
		13412	12616	8498
		13413	12618	8503
		13414	12620	8504
		13416	12625	8506
		13417	12626	8514
		13418	12631	8524
		13422	12635	8534
		13424	12638	8535
		13426	12682	8536
		13428	12683	8543
		13430	12684	8550
		13431	12716	8551
		13432	12718	8556
		13433	12720	8557
		13434	12740	8558
		13437	12742	8560
		13438	12744	8565
		13439	12751	8567
		13440	12752	8569
		13441	12753	8571
		13443	12798	8573
		13444	12800	8577
		13445	12816	8578
		13447	12832	8579
		13448	12834	8580
		13451	12836	8581
		13452	12856	8582
		13454	12876	8583
		13455	12932	8584

P-FC Values and Corresponding AAL Region Indices			
		12950	8586
		12990	8590
		12991	8597
		12992	8603
		13182	8604
		13220	8613
		13224	8614
		13236	8621
		13238	8622
		13252	8623
		13254	8625
		13262	8629
		13264	8648
		13266	8651
		13280	8653
		13288	8657
		13296	8658
		13297	8660
		13298	8665
		13300	8666
		13306	8667
		13310	8670
		13314	8673
		13316	8674
		13318	8681
		13323	8683
		13324	8689
		13327	8693
		13332	8700
		13336	8705
		13340	8730
		13342	8735
		13343	8736
		13347	8738
		13348	8746
		13350	8756
		13352	8766

P-FC Values and Corresponding AAL Region Indices			
		13354	8768
		13356	8775
		13358	8780
		13368	8782
		13369	8783
		13370	8788
		13378	8792
		13379	8798
		13380	8799
		13382	8800
		13384	8803
		13386	8805
		13387	8809
		13388	8810
		13390	8811
		13391	8815
		13392	8816
		13393	8932
		13394	8934
		13396	8941
		13398	8970
		13402	9021
		13404	9048
		13408	9063
		13411	9240
		13412	9280
		13413	9295
		13414	9353
		13415	9355
		13416	9431
		13417	9462
		13418	9470
		13422	9471
		13424	9472
		13426	9485
		13428	9495
		13430	9501

P-FC Values and Corresponding AAL Region Indices			
		13431	9505
		13432	9511
		13433	9512
		13434	9550
		13437	9551
		13438	9552
		13439	9574
		13440	9586
		13441	9587
		13443	9588
		13444	9599
		13445	9601
		13447	9633
		13448	9648
		13451	9663
		13452	9685
		13454	9688
		13455	9737
			9744
			9759
			9926
			9935
			9959
			9969
			9975
			9976
			9981
			10059
			10085
			10095
			10097
			10166
			10168
			10201
			10208
			10210
			10218

P-FC Values and Corresponding AAL Region Indices		
		10220
		10226
		10228
		10238
		10239
		10241
		10242
		10266
		10270
		10272
		10277
		10278
		10280
		10281
		10282
		10283
		10286
		10290
		10291
		10359
		10390
		10398
		10399
		10433
		10439
		10440
		10494
		10556
		10630
		10632
		10665
		10666
		10667
		10671
		10672
		10723
		10725

P-FC Values and Corresponding AAL Region Indices		
		10726
		10786
		10788
		10852
		10894
		10902
		10903
		10904
		10932
		10973
		11025
		11058
		11092
		11118
		11130
		11131
		11138
		11170
		11174
		11200
		11205
		11206
		11210
		11211
		11245
		11246
		11251
		11252
		11257
		11287
		11288
		11290
		11328
		11348
		11358
		11361
		11362

P-FC Values and Corresponding AAL Region Indices		
		11367
		11368
		11386
		11406
		11424
		11430
		11432
		11436
		11441
		11442
		11443
		11444
		11450
		11454
		11480
		11482
		11483
		11484
		11522
		11524
		11540
		11560
		11590
		11594
		11599
		11600
		11618
		11638
		11649
		11651
		11653
		11654
		11673
		11674
		11705
		11715
		11716

P-FC Values and Corresponding AAL Region Indices		
		11725
		11832
		11834
		11867
		11870
		11872
		11896
		11905
		11906
		11908
		11937
		11941
		11947
		11948
		11953
		11957
		12054
		12056
		12063
		12064
		12066
		12076
		12082
		12092
		12099
		12102
		12104
		12126
		12128
		12132
		12137
		12138
		12139
		12140
		12146
		12165
		12167

P-FC Values and Corresponding AAL Region Indices		
		12173
		12179
		12180
		12236
		12274
		12278
		12280
		12284
		12288
		12301
		12315
		12405
		12406
		12412
		12417
		12421
		12516
		12518
		12521
		12522
		12527
		12528
		12530
		12531
		12535
		12542
		12544
		12554
		12556
		12558
		12562
		12566
		12567
		12568
		12569
		12570

P-FC Values and Corresponding AAL Region Indices		
		12573
		12574
		12578
		12580
		12584
		12586
		12587
		12588
		12590
		12592
		12595
		12596
		12597
		12598
		12599
		12600
		12602
		12603
		12604
		12610
		12612
		12614
		12615
		12616
		12618
		12620
		12625
		12626
		12631
		12633
		12635
		12636
		12638
		12674
		12682
		12683
		12684

P-FC Values and Corresponding AAL Region Indices		
		12700
		12716
		12718
		12720
		12736
		12740
		12741
		12742
		12744
		12751
		12752
		12753
		12755
		12756
		12788
		12790
		12798
		12800
		12816
		12832
		12834
		12836
		12852
		12856
		12870
		12875
		12876
		12906
		12927
		12929
		12932
		12941
		12950
		12975
		12986
		12990
		12991

P-FC Values and Corresponding AAL Region Indices		
		12992
		13021
		13066
		13182
		13201
		13202
		13207
		13220
		13223
		13224
		13231
		13232
		13236
		13238
		13240
		13252
		13253
		13254
		13262
		13263
		13264
		13266
		13277
		13278
		13280
		13288
		13295
		13296
		13297
		13298
		13300
		13306
		13310
		13314
		13316
		13318
		13321

P-FC Values and Corresponding AAL Region Indices		
		13322
		13323
		13324
		13325
		13327
		13328
		13329
		13332
		13335
		13336
		13338
		13340
		13342
		13343
		13344
		13346
		13347
		13348
		13350
		13352
		13354
		13356
		13358
		13360
		13364
		13366
		13368
		13369
		13370
		13378
		13379
		13380
		13382
		13383
		13384
		13385
		13386

P-FC Values and Corresponding AAL Region Indices		
		13387
		13388
		13390
		13391
		13392
		13393
		13394
		13395
		13396
		13398
		13402
		13404
		13405
		13406
		13408
		13410
		13411
		13412
		13413
		13414
		13415
		13416
		13417
		13418
		13420
		13422
		13424
		13426
		13428
		13430
		13431
		13432
		13433
		13434
		13437
		13438
		13439

P-FC Values and Corresponding AAL Region Indices		
		13440
		13441
		13442
		13443
		13444
		13445
		13447
		13448
		13451
		13452
		13454
		13455

GLOSSARY

fMRI functional magnetic resonance imaging.

FC functional connectivity.

DFC dynamic functional connectivity.

GWI Gulf War illness.

PTSD Post Traumatic Stress Disorder

BOLD Blood oxygen level dependent.

RCNN Region based convolutional neural network

SVM Support Vector Machine

4-D four dimensional

ICA Independent Component Analysis

GICA Group ICA

PCA Principal component analysis

LDA Linear Discriminant Analysis

SVM Support Vector Machine

AAL Automated Anatomical Labeling

TTEST2 Two sample ttest with pooled or unpooled variance estimates.